NASA
SPACE VEHICLE
DESIGN CRITERIA
(STRUCTURES)

NASA SP-8072

ACOUSTIC LOADS GENERATED BY THE PROPULSION SYSTEM

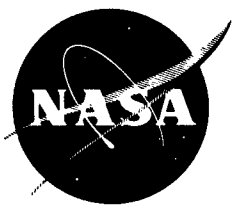

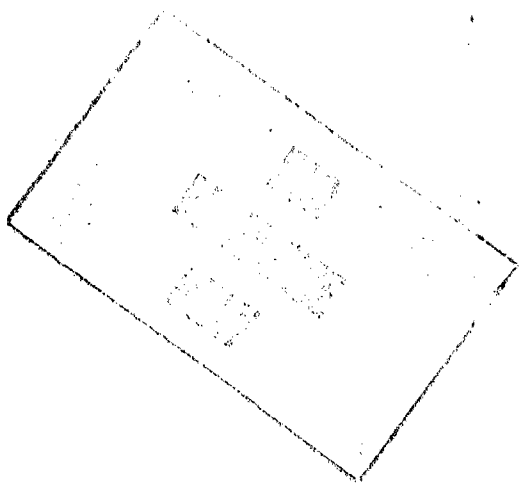

JUNE 1971

NATIONAL AERONAUTICS AND SPACE ADMINISTRATION

FOREWORD

NASA experience has indicated a need for uniform criteria for the design of space vehicles. Accordingly, criteria are being developed in the following areas of technology:

Environment
Structures
Guidance and Control
Chemical Propulsion

Individual components of this work will be issued as separate monographs as soon as they are completed. A list of all published monographs in this series can be found at the end of this document.

These monographs are to be regarded as guides to the formulation of design requirements and specifications by NASA centers and project offices.

This monograph was prepared under the cognizance of the Langley Research Center. The Task Manager was G. W. Jones, Jr. The author was K. M. Eldred of Wyle Laboratories. A number of other individuals assisted in planning the monograph, developing the material, and reviewing the drafts. In particular, the significant contributions made by C. M. Ailman, C. P. Berry, and D. L. Keeton of McDonnell Douglas Corporation; D. A. Bies of Bolt Beranek & Newman Incorporated; D. A. Bond of Advance Graphic Systems, Incorporated; P. M. Edge, Jr., of NASA Langley Research Center; H. Himelblau and C. L. Stevens of North American Rockwell Corporation; R. C. Potter of Wyle Laboratories; R. H. Lyon of Massachusetts Institute of Technology; D. L. Smith of the Air Force Flight Dynamics Laboratory; P. H. White of Measurement Analysis Corporation; and K. J. Young of The Boeing Company are hereby acknowledged.

NASA plans to update this monograph when need is established. Comments and recommended changes in the technical content are invited and should be forwarded to the attention of the Design Criteria Office, Langley Research Center, Hampton, Virginia 23365.

June 1971

GUIDE TO THE USE OF THIS MONOGRAPH

The purpose of this monograph is to provide a uniform basis for design of flightworthy structure. It summarizes for use in space vehicle development the significant experience and knowledge accumulated in research, development, and operational programs to date. It can be used to improve consistency in design, efficiency of the design effort, and confidence in the structure. All monographs in this series employ the same basic format – three major sections preceded by a brief INTRODUCTION, Section 1, and complemented by a list of REFERENCES.

The STATE OF THE ART, Section 2, reviews and assesses current design practices and identifies important aspects of the present state of technology. Selected references are cited to supply supporting information. This section serves as a survey of the subject that provides background material and prepares a proper technological base for the CRITERIA and RECOMMENDED PRACTICES.

The CRITERIA, Section 3, state *what* rules, guides, or limitations must be imposed to ensure flightworthiness. The criteria can serve as a checklist for guiding a design or assessing its adequacy.

The RECOMMENDED PRACTICES, Section 4, state *how* to satisfy the criteria. Whenever possible, the best procedure is described; when this cannot be done, appropriate references are suggested. These practices, in conjunction with the criteria, provide guidance to the formulation of requirements for vehicle design and evaluation.

CONTENTS

1. INTRODUCTION 1

2. STATE OF THE ART 3

2.1 Rocket-Exhaust Noise Generation 3
2.1.1 Overall Sound Power and Acoustic Efficiency 6
2.1.2 Sound-Power Spectrum 8
2.1.3 Directional Characteristics 10
2.1.4 Noise Generation Along the Exhaust Flow 12
2.1.5 Combustion Effects 15
2.1.6 Summary of Significant Noise-Generation Parameters 15
2.2 Vehicle Loading 16
2.3 Prediction Methods for Near-Field Noise 19
2.3.1 Empirical Analysis 19
2.3.2 Experimental Determination 23
2.4 Minimizing the Acoustic Loads 23

3. CRITERIA 24

3.1 Acoustic-Load Parameters 25
3.2 Prediction of Acoustic Loads by Empirical Analysis 25
3.3 Testing 26
3.3.1 Subscale Model Tests 26
3.3.2 Full-Scale Tests 27
3.4 Minimizing the Acoustic Loads 27

4. RECOMMENDED PRACTICES 27

4.1 Acoustic-Load Parameters 27
4.2 Prediction of Acoustic Loads by Empirical Analysis 28
4.3 Testing 32
4.3.1 Subscale Model Tests 32
4.3.2 Full-Scale Tests 33
4.4 Minimizing the Acoustic Loads 34

APPENDIX Definitions of Acoustical Terminology 35

REFERENCES 39

SYMBOLS 43

NASA SPACE VEHICLE DESIGN CRITERIA
MONOGRAPHS ISSUED TO DATE 47

ACOUSTIC LOADS GENERATED BY THE PROPULSION SYSTEM

1. INTRODUCTION

A space vehicle is subjected to a severe fluctuating external-pressure loading when its rocket-propulsion system is operated in the atmosphere. Such acoustic loading* is described in terms of its overall sound-pressure level* and its frequency spectrum and spatial correlation* as functions of position over the vehicle's surface. The acoustic loading results from the broad frequency-spectrum acoustic field generated by the mixing of the rocket-engine exhaust stream with the ambient atmosphere. Acoustic loads are a principal source of structural vibration and internal noise during launch or static-firing operations but do not generally present a critical design condition for the main load-carrying structure. However, acoustic loads may be critical to the proper functioning of vehicle components and their supporting structures, which are otherwise lightly loaded. The prediction of acoustic loading is essential to provide a necessary input for the determination of vibration loads throughout the vehicle, and for the development of the vibration-test specifications and the associated dynamic design requirements which are necessary to ensure overall vehicle reliability.

Potential problems which may result from acoustic loading include:

- Malfunction of electronic and mechanical components in the vehicle (from structural vibration and internal acoustic loading)
- Fatigue failure of internal components and supporting hardware, such as cable-bundle supports, instrument-mounting brackets, and distributed piping systems (from structural vibration)
- Fatigue of lightweight exterior structures, such as aerodynamic fins and antenna panels (from direct external acoustic loading)
- Fatigue of lightweight spacecraft structures (from internal acoustic noise and structural vibration)
- Adverse environmental conditions for vehicle occupant

*See Appendix for definitions

This monograph is concerned primarily with predicting loads generated on the vehicle by rocket-propulsion systems and secondarily with minimizing the sound field, where necessary. It excludes prediction of internal acoustic loads and loads resulting from nonacoustic sources of structural vibratory responses, such as impingement by the exhaust streams of control rockets and aerodynamically induced loads.

The maximum acoustic loading from the rocket occurs on the vehicle during test-stand firings or liftoff. During launch, loading decreases as the vehicle accelerates. When the vehicle's velocity exceeds the speed of sound, the propulsion-induced acoustic loading over most of the vehicle is reduced to zero because the sound generated aft of the vehicle by the rocket's exhaust is propagated forward at a velocity less than that of the vehicle. In the supersonic regime, however, there may be a relatively low-level acoustic loading from the rocket in the vehicle's base region resulting from propagation of noise through the vehicle's wake.

The principal parameters affecting acoustic loading are:

- Rocket-nozzle exit-flow parameters
- Vehicle, stand, and flow geometry
- Vehicle velocity

The primary source of the acoustic field is the fluctuating turbulence in the mixing region of the rocket-exhaust flow. Since this mixing region surrounds the exhaust flow over its entire length, the noise source extends over a great distance. Noise generated by the rocket is a function of the properties of the turbulent flow, which, in turn, are related to the mean flow parameters and geometry. Noise is radiated in all directions from the flow; however, the magnitude of the acoustic field is highly directional; the angle of maximum radiation for existing chemical rockets is about 50 degrees from the direction of the flow. For a given rocket flow, the acoustic loading on the vehicle is therefore greater when the flow is directed at right angles to the vehicle's axis (as on a test stand or at liftoff) than when it is directed aft along the axis (as in flight). Acoustic loading on the vehicle generally decreases as distance from the rocket flow increases, and is affected by nearby reflecting objects.

Additional noise sources in the rocket flow may be of importance for certain engine-vehicle-deflector configurations. These sources include interaction of flow turbulence with the deflector surfaces and with shock waves associated with the deflector, and oscillating flame fronts which result from reignition of exhaust gases downstream of the nozzle.

Accurate analytical prediction of the acoustic loading at a specified point on the vehicle at a given time of operation is virtually impossible because of many complicating factors. Therefore, the approach to prediction presented in this monograph is based on analysis of experimental data.

The response of the space-vehicle structure to acoustic loading is treated in the monograph on structural vibration prediction (ref. 1). Also, the related topic of aerodynamic-pressure-field fluctuations (similar to acoustic loading because they can cause similar problems in space-vehicle design) is partially covered in the monograph on buffeting during atmospheric ascent (ref. 2).

2. STATE OF THE ART

Prediction of the acoustic loads on space vehicles that are generated by the propulsion system requires the use of analytical methods (based on experimental data) supplemented by tests. In general, current prediction methods are useful only for analysis of chemical rockets where nozzle design, exhaust-flow characteristics, and deflector configuration are typical of engines and deflectors presently in use. Where new engine or deflector designs are proposed which significantly depart from existing configurations, model and full-scale experimental programs are necessary to obtain the acoustic loading on the structure, as needed for proper design of the structure.

2.1 Rocket-Exhaust Noise Generation

The characteristics of rocket noise may be summarized in the following manner. The acoustic (sound) power generated by a supersonic rocket exhaust is directly proportional to the cube of the exhaust velocity. The spectrum of the noise generated is broadband in nature; no discrete frequency sound is normally observed, and the spectrum peak frequency is inversely proportional to the size of the engine. Noise is radiated in all directions, but the maximum radiation is at an acute angle to the exhaust-flow direction. The noise is generated over an extended source region throughout the entire length of the exhaust-mixing flow, as illustrated in figure 1. The principal source of the noise is in the subsonic flow, downstream of the supersonic core of the jet; the predominant angle of maximum noise radiation is approximately 50 to 70 degrees from the axis of the flow, depending on the exhaust-flow parameters.

Knowledge of the characteristics of rocket-exhaust noise has been obtained principally from experiments. However, theory extended from original low-speed work (refs. 3 and 4) to supersonic flow (ref. 5) has played an important role in the development of the understanding of the complex process of the noise generated by high-speed jet-exhaust gases mixing with the atmosphere. References 6 and 7, which are summary

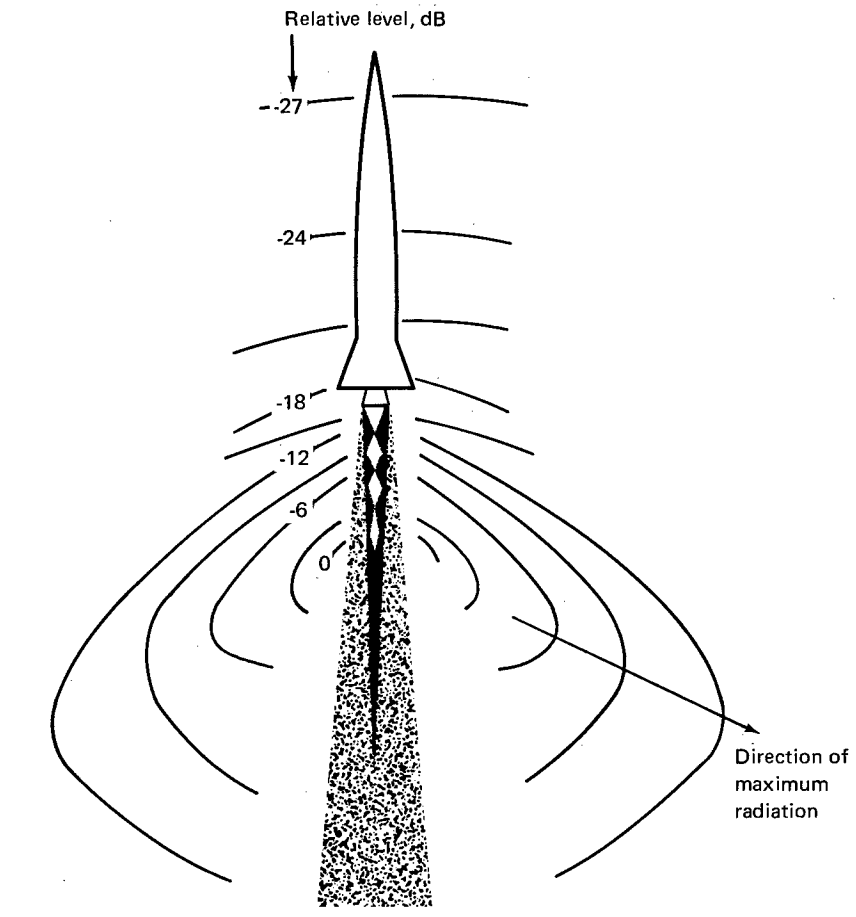

(a) In flight

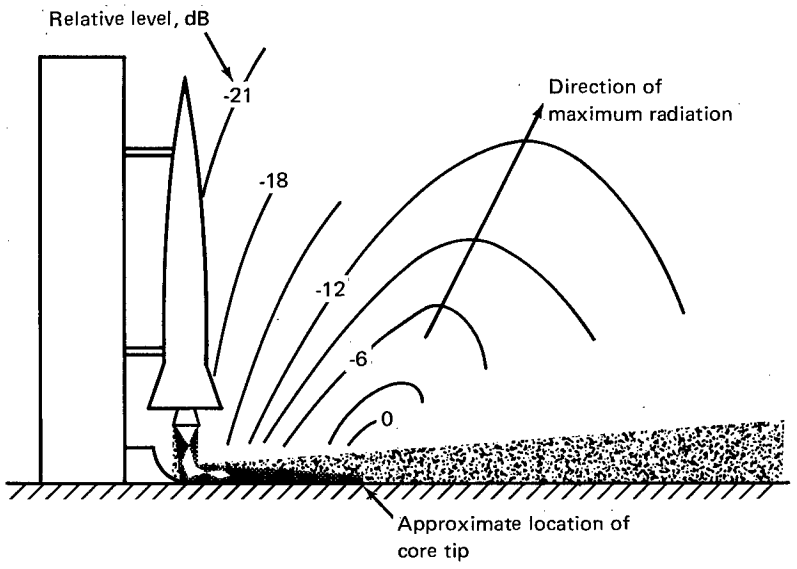

(b) At launch

Figure 1. – Sketch of the rocket flow and contour of equal overall sound-pressure level for flight and launch cases.

papers, and reference 8, present reviews of the theoretical aspects of jet-noise generation.

The most productive approach to the understanding and prediction of rocket-exhaust noise has been achieved by applying similarity principles and parameters to experimental data. Similarity concepts for jets are discussed extensively in reference 9 and extended to rockets in references 10 to 13. The basic premise is that the noise field for rockets is similar when the exhaust flow is similar.

The most elementary similarity application is that of comparing the noise field from two geometrically similar jets or rockets having identical nozzle-flow parameters and differing only in size. In this case (fig. 2), the overall sound-pressure level is identical at locations that are geometrically similar throughout the noise field. However, the spectrum is shifted in frequency so that the parameter frequency times nozzle diameter, fd, remains constant. This relationship, supplemented by theory for low-speed jets (refs. 3 to 8) and experimental data (refs. 9 to 11 and 14), has led to general use of the nondimensional Strouhal number, fd/U, where U is velocity, as the principal similarity parameter for jet- and rocket-noise spectra.

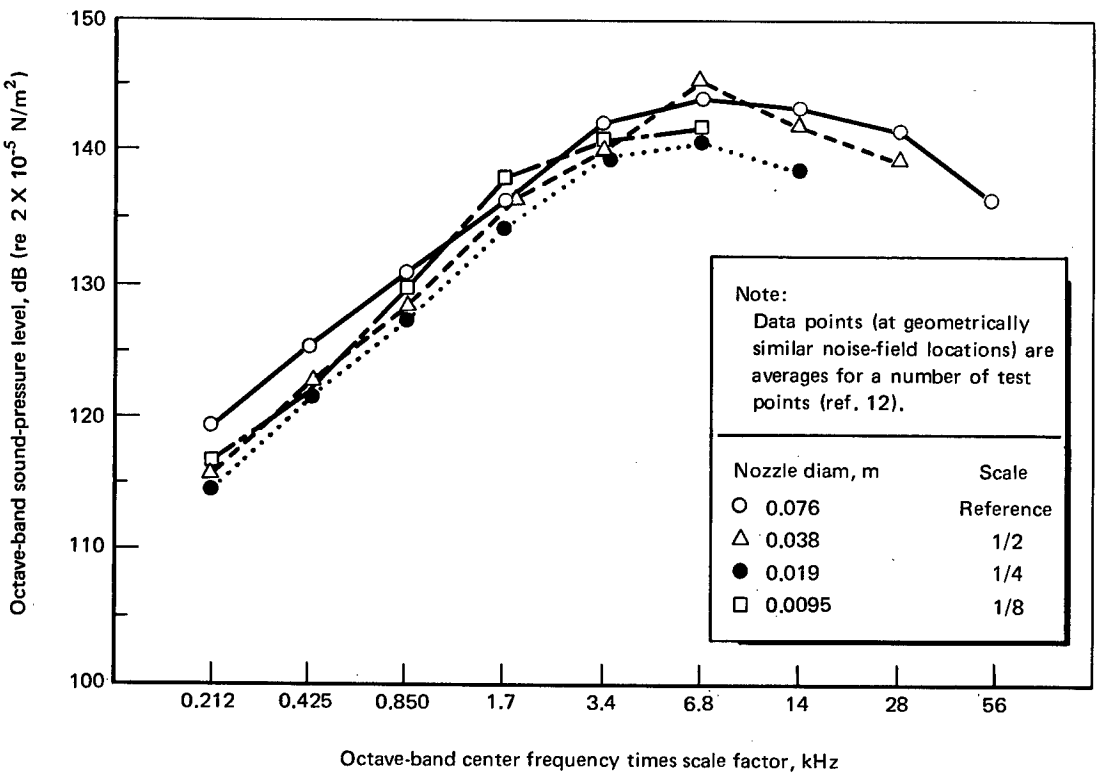

Figure 2. – Similarity of noise produced by four nozzles of different diameters, all operating at the same plenum condition.

The use of other similarity parameters is best demonstrated by examining various features of the rocket-noise field for undeflected single-nozzle chemical rockets, where most data are available, supplemented by data for special cases of clustered nozzles, deflectors, and nonchemical rockets.

2.1.1 Overall Sound Power and Acoustic Efficiency

The overall sound-power level for undeflected rocket exhausts is summarized in figure 3, which presents data from references 15 to 23. The data include both solid- and liquid-fueled chemical rockets in the thrust range of 1.56 to 31 100 kN (350 to 7 000 000 lb), together with a few examples of clustered nozzles and nuclear-powered hydrogen supersonic jets. The acoustic efficiency, defined as the ratio of the sound

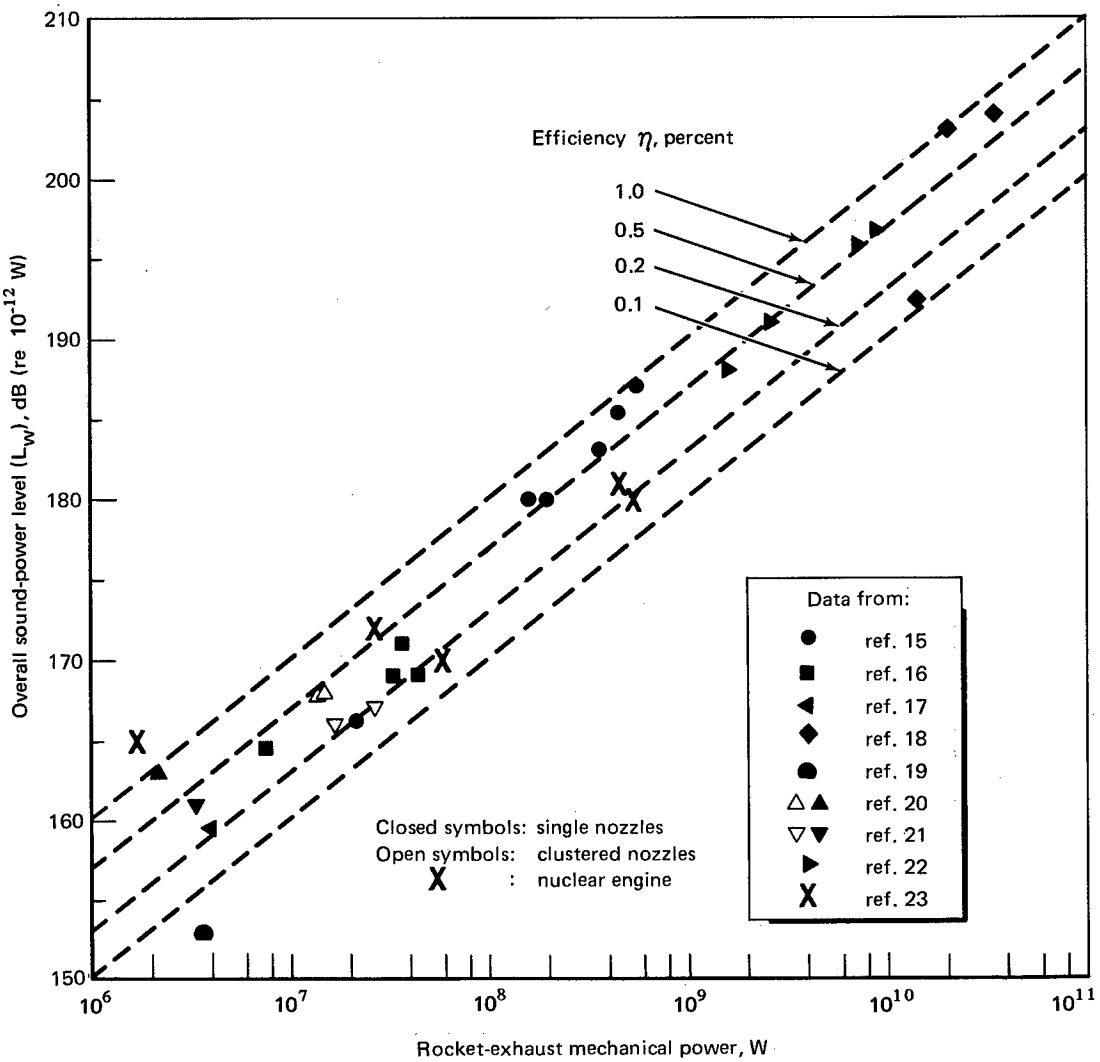

Figure 3. – Overall sound-power level for solid- and liquid-fueled undeflected rockets, including a thrust range of 1.56 to 31 100 kN (350 to 7 000 000 lb).

power to the rocket exhaust's mechanical power, for the majority of these data range between 0.2 and 1.0 percent; however, an earlier empirical-prediction method that had widespread use showed the sound power proportional to the exhaust's mechanical power raised to a power of 1.35 (ref. 15). Although this relationship appeared correct for the data available at that time for rockets ranging in thrust from 4.45 to 580 kN (1000 to 130 000 lb), it does not appear to apply to higher thrust rockets. Also, more recent data on low-thrust rockets show acoustic efficiencies in the same range as the high-thrust rockets. One of the principal reasons may be that the acoustic instrumentation for the more recent data had a frequency response more compatible with the spectrum. It is concluded that the acoustic efficiency is a constant for undeflected rocket exhausts with similar nozzle-flow parameters, with 0.5 percent as the most probable value and 1.0 percent as a conservative upper bound.

The acoustic efficiency of deflected rocket exhausts is less than that of undeflected rockets (fig. 4, by data from ref. 17). The differences are greatest when the exhaust impinges on a flat plate which is normal to the flow and are least for rockets that are deflected by smoothly curved buckets. This decrease in efficiency is considered to be caused by the modification of the exhaust flow by the deflector-nozzle configuration.

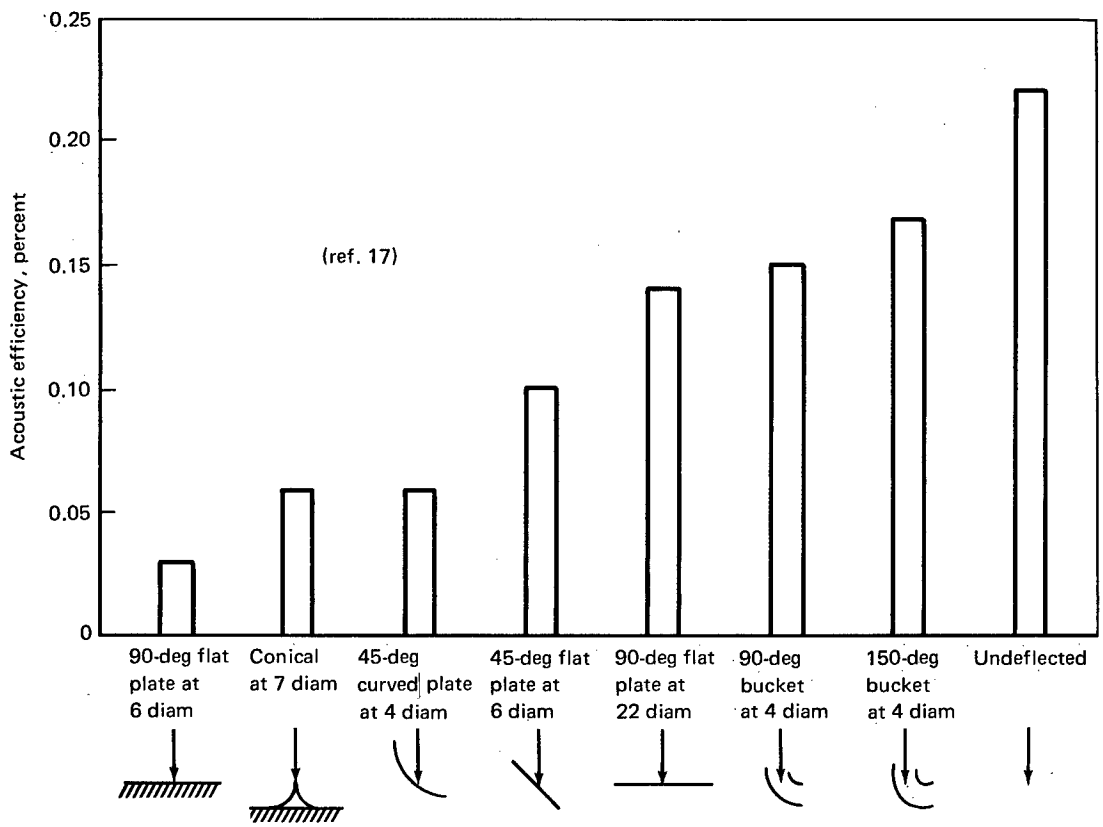

Figure 4. – Acoustic efficiency of various deflected rockets.

2.1.2 Sound-Power Spectrum

A sound-power spectrum for chemical rockets is given in figure 5, with data from references 15 to 18, 20, and 24. The data are primarily from undeflected rocket exhausts but include data from aerodynamically smooth bucket deflectors, which were seen in figure 4 to have efficiencies similar to those of the undeflected exhausts. The normalizing parameter, U_e/d_e in the quantity $W(f)U_e/W_{OA}d_e$, adjusts the measured relative sound power per Hz $W(f)/W_{OA}$ to relative power per unit Strouhal number so that the data are comparable and the area under the curve is unity. The scatter in the data shows the accuracy limitations to be expected when the faired curve is used to predict the sound-power spectrum of a new but similar chemical rocket.

The power spectrum of chemical rockets (fig. 5) covers a wide frequency range, with the maximum at a Strouhal number of approximately 0.02. However, when data for supersonic hydrogen-exhaust flows (refs. 21 and 23) are compared with those of chemical rockets as shown in figure 6, their power spectra are observed to reach a maximum at significantly lower values of Strouhal number than 0.02. The curve of figure 5 is limited to chemical rockets with an exit exhaust velocity in the range of

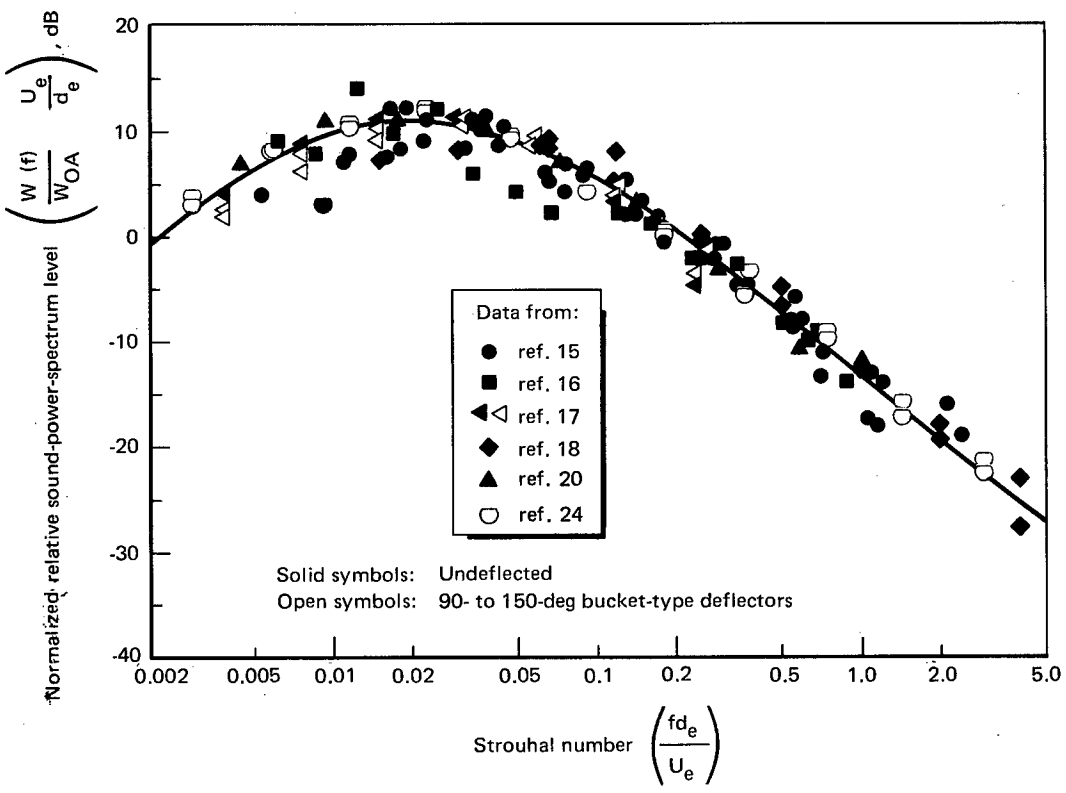

Figure 5. – Normalized relative power spectrum as a function of Strouhal number for standard solid- and liquid-fueled chemical rockets with single nozzles, including a thrust range of 1.56 to 31 100 kN (350 to 7 000 000 lb).

1800 to 2600 m/sec (5900 to 8600 ft/sec) as compared with the 3700- to 5800-m/sec (12 200 to 19 000 ft/sec) values for the hydrogen-exhaust flows of figure 6.

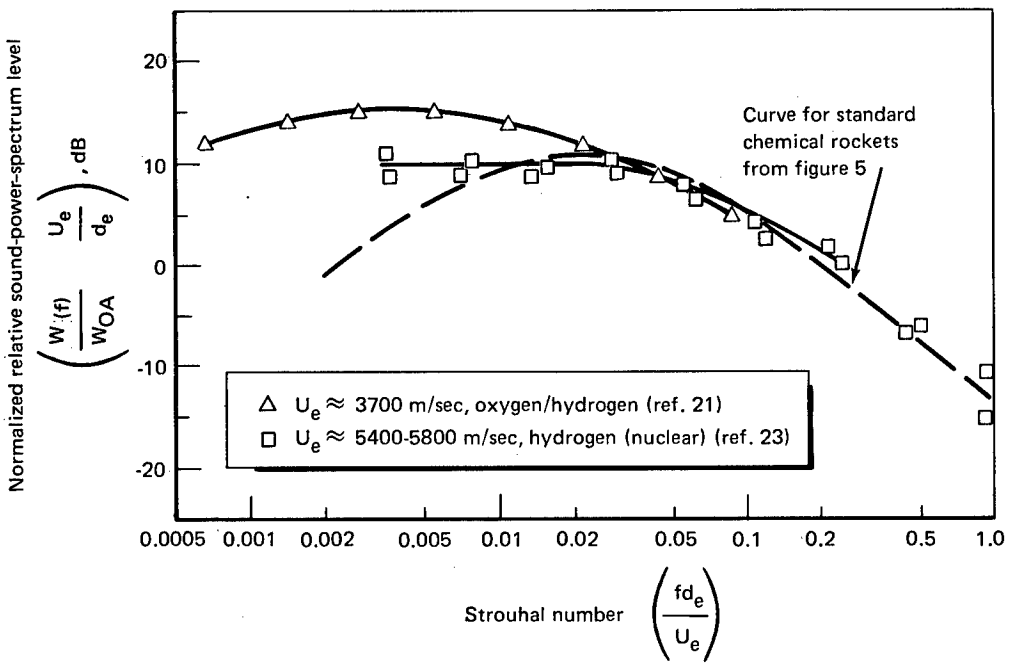

Figure 6. – Normalized relative sound-power spectrum as a function of Strouhal number for two examples of undeflected hydrogen rockets compared with standard chemical rockets.

Comparisons of power spectra for examples of clustered nozzles and a single nozzle are given in figure 7 for each of the two exhaust regimes of figures 5 and 6. Both examples show a good data fit when the Strouhal number of the cluster is based on a diameter of a single nozzle having an exit area equal to the total exit area of the cluster. In both cases, the nozzles are judged to be so close that the noise results primarily from the combined flow. If the nozzles should be spaced farther apart, the noise spectra could be affected by both the individual flows and the combined flow (refs. 10 and 21). Experimental evidence (ref. 24) also suggests that when the exhaust flow is deflected, the simplest approach to dealing with multiple nozzles is to use the equivalent diameter of a single nozzle having an exit area equal to the combined areas of the multiple nozzles, since the deflector will cause the flows to mix rapidly, thus producing a combined single flow. This effect is well demonstrated by the data (ref. 24) for full-scale deflected flows from the eight-engine Saturn booster (fig. 5).

Figure 8 shows a few examples from reference 17 of the normalized power spectra from rockets that were exhausted into other types of deflectors, which result in much greater changes in the flow than those associated with a simple bucket deflector. These deflectors cause a reduction of overall sound power (fig. 4) and produce marked

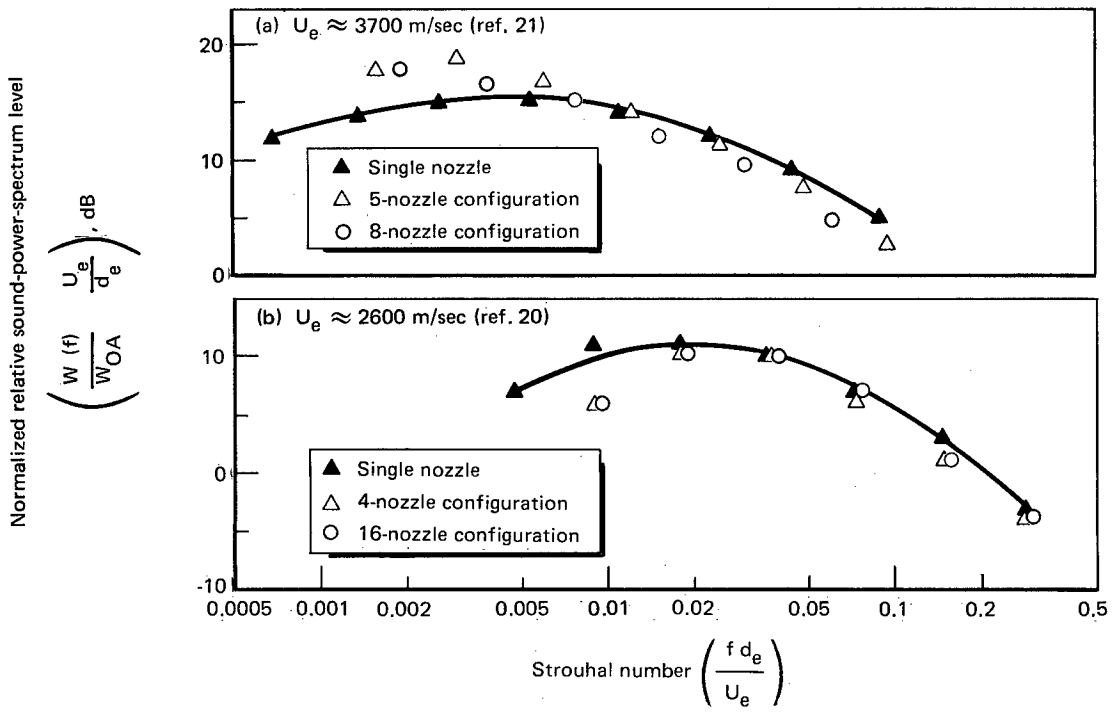

Figure 7. – Comparison of normalized relative sound-power spectrum for examples of clustered rockets in two exhaust-flow velocity regimes, with the spectrum for single-nozzle rockets in the same velocity regime.

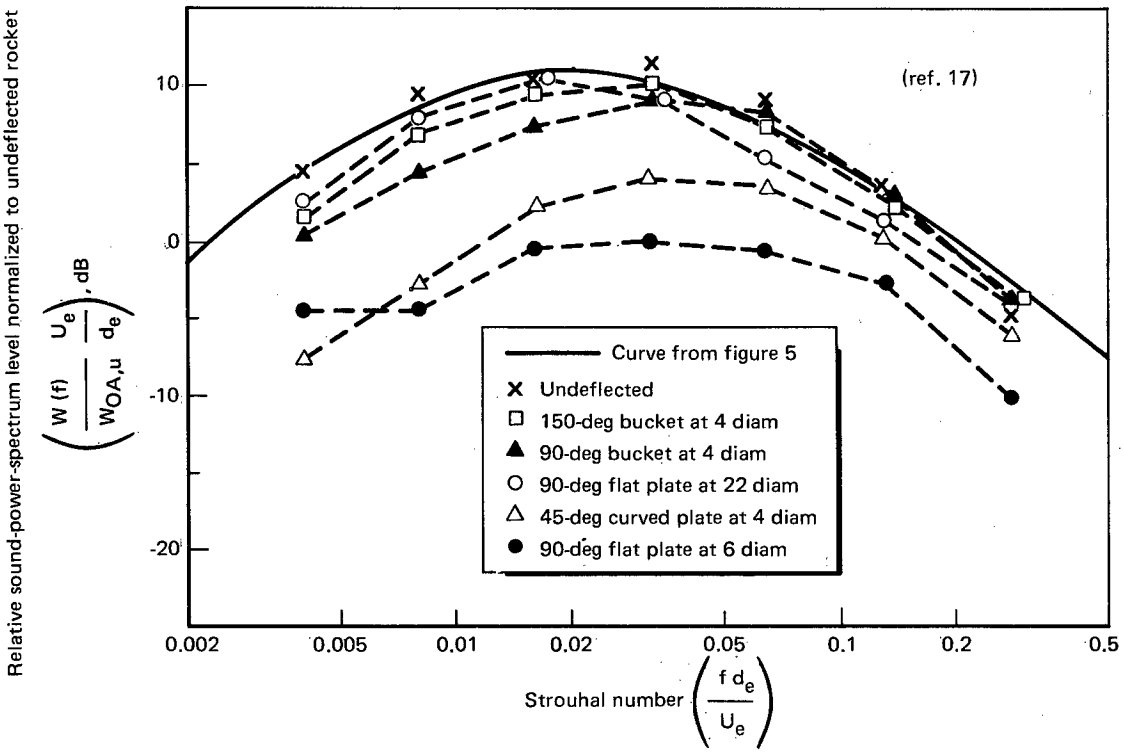

Figure 8. – Examples of the effect of various deflector configurations on the acoustic-power spectrum, normalized to the undeflected rocket.

changes in the power spectrum. Consequently, the general relationships for power (fig. 3) and spectra (fig. 5) may be invalid whenever the deflector geometry differs significantly from an aerodynamically clean open-bucket design.

2.1.3 Directional Characteristics

The directional characteristics for the overall sound-pressure levels of various jets and rockets are illustrated in figure 9. The angle of maximum radiation relative to the exhaust axis increases as the speed of sound in the flow increases. This effect is believed to result from refraction of sound as it is transmitted through the shear layer into the exhaust-gas flow (refs. 9, 25, and 26). Note that the results for the higher speed hydrogen rockets are dissimilar to those for the typical chemical rockets.

The directional characteristics of the sound are also functions of frequency, as illustrated for chemical rockets in figure 10, using data from references 13, 15, 17, and 27. In general, the directional characteristics for the frequencies at higher values of Strouhal number reach maxima at the angle predicted from simple refraction theory (refs. 9 and 10), whereas the maxima for lower frequency sound are at more acute angles to the axis. This effect is believed to result because low frequencies are not

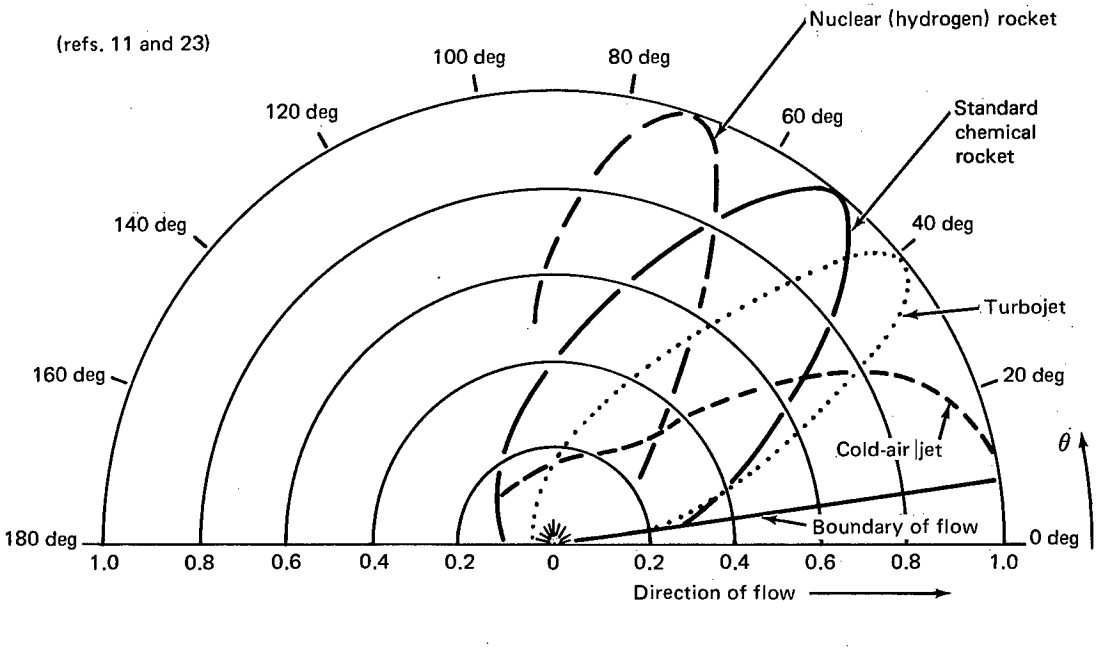

Figure 9. – Far-field directional characteristics of the overall sound-pressure level for four types of jet flow.

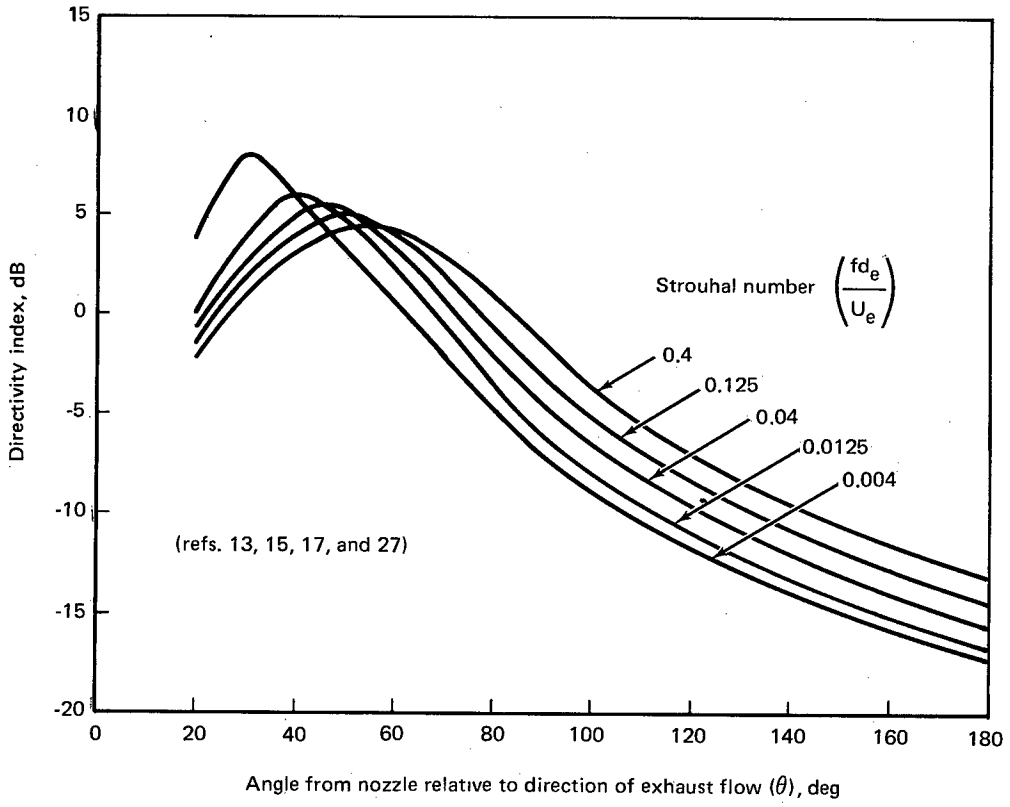

Figure 10. – Directivity of far-field noise for standard chemical rockets for several values of Strouhal number.

refracted as much as the higher frequencies because their wavelengths are much longer in comparison to the width of the shear layer; and, from Mach number and convection effects on the low frequencies (refs. 5 to 9).

2.1.4 Noise Generation Along the Exhaust Flow

The previous discussions have summarized the extent and limitations of similarity relationships for the total sound field from a rocket exhaust. For the prediction of acoustic loading at positions close to the rocket flow, it is necessary to examine the distribution of noise along the exhaust stream. The length of the supersonic core of a rocket exhaust appears to be directly related to the fully expanded exit Mach number, M_e, as shown by the data in figure 11. The rocket data in this figure are from reference 28. Estimates of the relative overall-sound-power per unit-core-length have been calculated from noise measurements along the flow (refs. 10 and 29), and are given in figure 12. The maxima are at distances ranging between one and two core lengths. It should be noted that results of this type can be calculated for only sonic and supersonic jets (refs. 9 and 10), where the near-field hydrodynamic-convection effects associated with subsonic flows (ref. 30) are of little consequence.

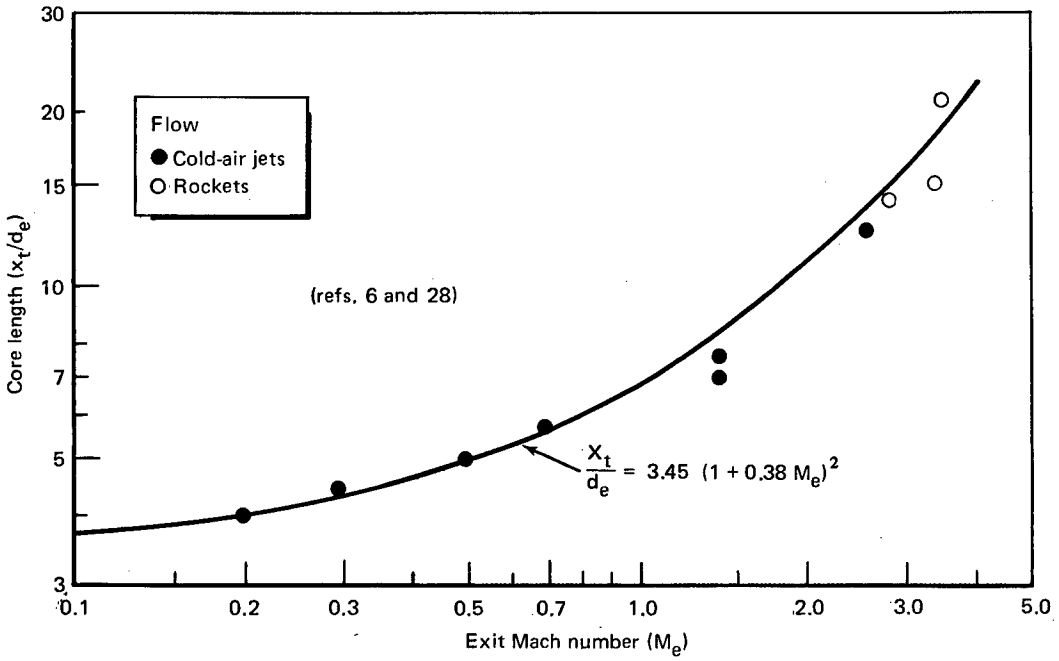

Figure 11. – Variation in core length for cold-air jets and standard chemical rockets as a function of nozzle-exit Mach number.

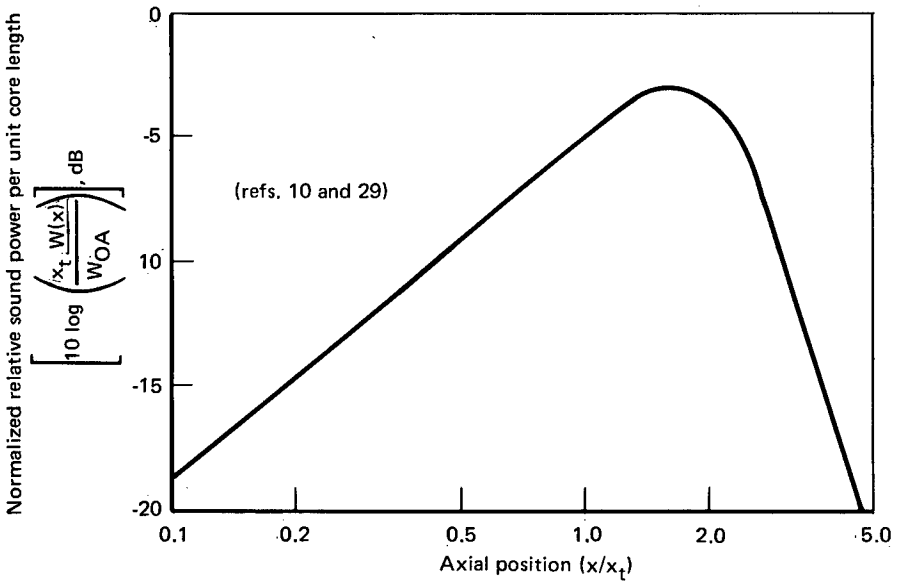

Figure 12. – Source-power distribution for standard chemical rockets.

Normalized power spectra for chemical rockets are summarized in terms of an axial Strouhal number in figure 13, in accordance with the technique of references 9 and 10. The scatter at low frequencies is partially due to the limited available data. In addition, scatter may result from a possible lack of similarity in the velocity distribution in the transition-mixing region along a supersonic core.

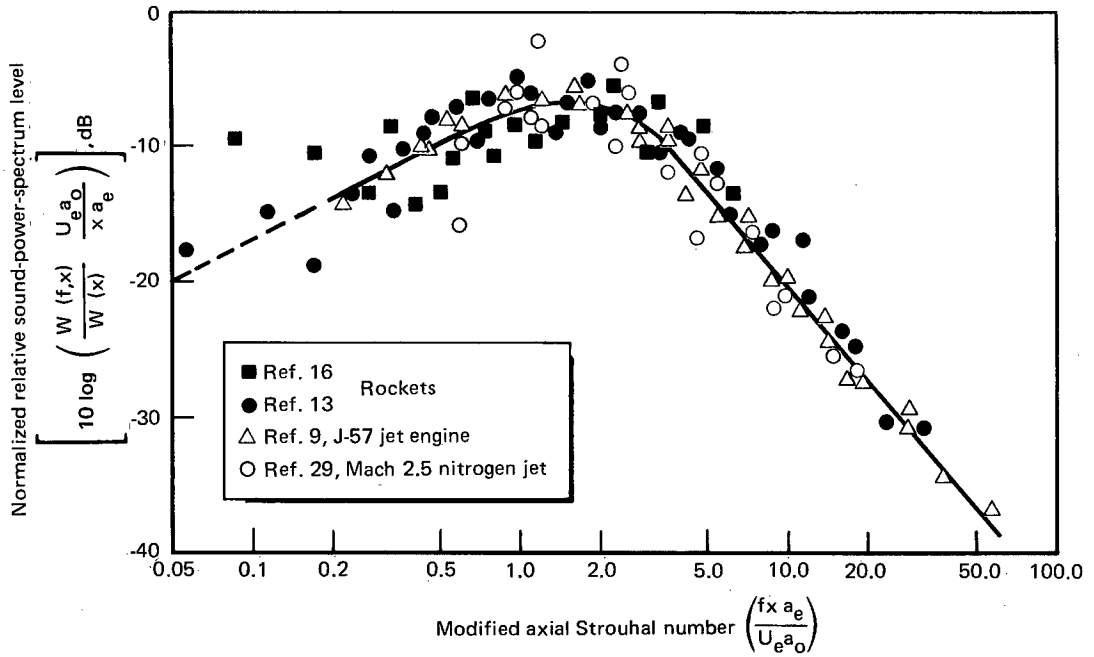

Figure 13. – Normalized relative power-spectrum level as a function of axial position along the flow for chemical rockets and jets.

To predict near-field sound-pressure levels from figures 12 and 13, a local directivity of sound radiation is required to give the distribution of sound radiated in each direction; however, direct experimental data do not exist for rockets in the form derived in reference 9 for sonic jets. Theory is not particularly helpful because the mechanism of directivity has not been fully confirmed for high-speed jet flows; both convection of the sources and refraction of the sound by the jet are considered responsible, but the significance of each has not been defined (refs. 25 and 26). Therefore, it is customary to apply the far-field directivity results such as those in figure 10 in predicting near-field acoustic levels from the power spectra derived along the flow.

An earlier approach to distributing the sources of the total acoustic-power spectrum along the flow is illustrated in figure 14 (data from references 13, 21, and 31). Here, for undeflected flows, the apparent location of the source of noise in each frequency band has been determined by fitting data measured along a simulated vehicle to an inverse-square loss curve and extrapolated to zero distance. For deflected flow, the distances were estimated from correlation measurements along a simulated vehicle. Since it is not possible to account for shielding, as can be accomplished with the distributions of figures 12 and 13, this approach may be used for predicting the noise of similar configurations only when no obstructions interfere with a line of sight between the vehicle and the flow.

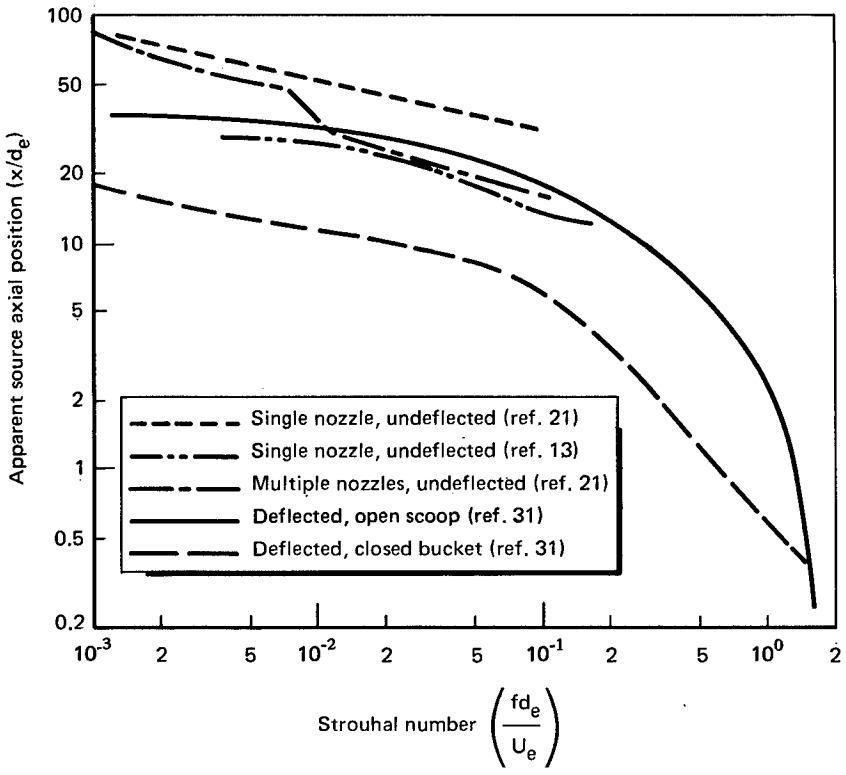

Figure 14. – Axial location of apparent sources as a function of Strouhal number for chemical rockets.

2.1.5 Combustion Effects

When there is combustion in the exhaust flow, it can cause additional noise. This effect has been associated with solid-fueled rockets (ref. 15) and with nuclear-rocket engines where the gaseous-hydrogen exhaust burns during ground test (ref. 23). Most chemical liquid-fueled engines burn slightly fuel rich, with some resulting combustion in the exhaust plume. Reference 32 indicates that the combustion of fuel-rich exhaust causes an increase of 2 to 14 dB in low-frequency noise; however, these measurements are close to the exhaust stream, and the increases may not be found at greater distances (ref. 15). The general effects of combustion are further complicated by the nature of the flame front thus formed. Reference 15 indicates that an increase of 2 to 4 dB found at locations near the nozzle at the lower frequencies was a result of the oscillation of the flame front, which disappeared when the flame front was stabilized.

2.1.6 Summary of Significant Noise-Generation Parameters

From the similarity relationships previously discussed and from reference 12, the following parameters are significant in scaling rocket noise:

- Exhaust-flow properties

  (a) Jet-exit velocity

  (b) Jet-exit Mach number

  (c) Jet-exit density

  (d) Jet-exit static pressure

- Configuration variables

  (a) Nozzle-exit diameter, shape, and area ratio

  (b) Multiple-nozzle geometry

  (c) Deflector geometry, including distance between nozzle and deflector

  (d) Exhaust-shroud geometry

  (e) Reflecting-surface geometry

- Ambient-atmospheric parameters

  (a) Pressure

  (b) Temperature

  (c) Gas Composition

2.2 Vehicle Loading

The minimum description of the loading on the vehicle, needed to estimate the structural response, is given in terms of the detailed distribution on the structure of the sound-pressure spectrum. A more detailed description also requires the spatial correlation pattern of the sound-pressure field to enable more exact vibration prediction. Such analyses are required for examining certain types of failures, such as the sonic fatigue of lightweight external panels.

Scattering from local structures, such as the launch or test stands, as well as from the vehicle structure itself, affects the radiated sound field from the exhaust flow. A deflector will normally cause an unsymmetrical loading in the vehicle, with a higher

level of loading measured on surfaces facing the deflected exhaust flow. The theory of scattering is complicated (ref. 33), but it may be used with certain assumptions to predict acoustic-load levels on the vehicle surface (ref. 34). However, in a complex configuration with many reflective surfaces nearby, the levels can be changed considerably and increased locally.

The maximum acoustic loading from the rocket exhaust occurs during ground firings when the vehicle is held static in a test stand or is starting to lift off from a launch stand. For standard ground-firing configurations, the flow is deflected by impinging perpendicularly on the ground plane or deflected to the side by a curved deflector (scoop or bucket). Although the deflector may reduce the total acoustic power, it often brings the exhaust flow closer to the vehicle, increasing the noise level over the vehicle. This effect is illustrated in figure 1 for a flow deflected at 90 degrees to the vehicle axis. Here the contours of equal sound-pressure level are shown to rotate with the flow (fig. 1b), placing the vehicle in a region of noise levels higher than those of the undeflected flow (fig. 1a).

A quantitative illustration of the increase of noise on the vehicle because of flow deflection is shown in figure 15 (taken from ref. 17). The figure shows the increase in sound-pressure level as a function of frequency at two positions on the vehicle. This increase in level is relative to the sound-pressure level measured at the same positions as when the flow was undeflected. From these examples it can be seen that the increase resulting from flow deflection is significant and is a function of position on the vehicle, distance from the nozzle to the deflector, type of deflector, and frequency.

During launch, increased loading from flow deflection has a significant effect until the distance between the nozzle and deflector is at least several core lengths (70 to 100 nozzle-exit diameters). When this distance is reached, most of the noise is generated in the undeflected exhaust flow. Further, the increase in distance between the vehicle and the deflector decreases the loading as a result of the inverse square loss. At greater distances the flow may be considered undeflected with respect to its noise generation.

Acoustic loading also decreases as the vehicle gains velocity (refs. 11 and 35). As shown in figure 16, when the vehicle reaches sonic velocity, the acoustic loading from the rocket exhaust decreases to an insignificant value since the vehicle's speed exceeds the propagation velocity of the exhaust noise. However, in the supersonic regime, a relatively low-level acoustic loading in the vehicle's base region may result from propagation of noise through the vehicle's wake.

The frequency-dependent spatial correlation is a measure of the distance over which the sound pressure may be considered in phase. It is important because spatial matching of pressure phase and response-displacement phase dictates the amount of

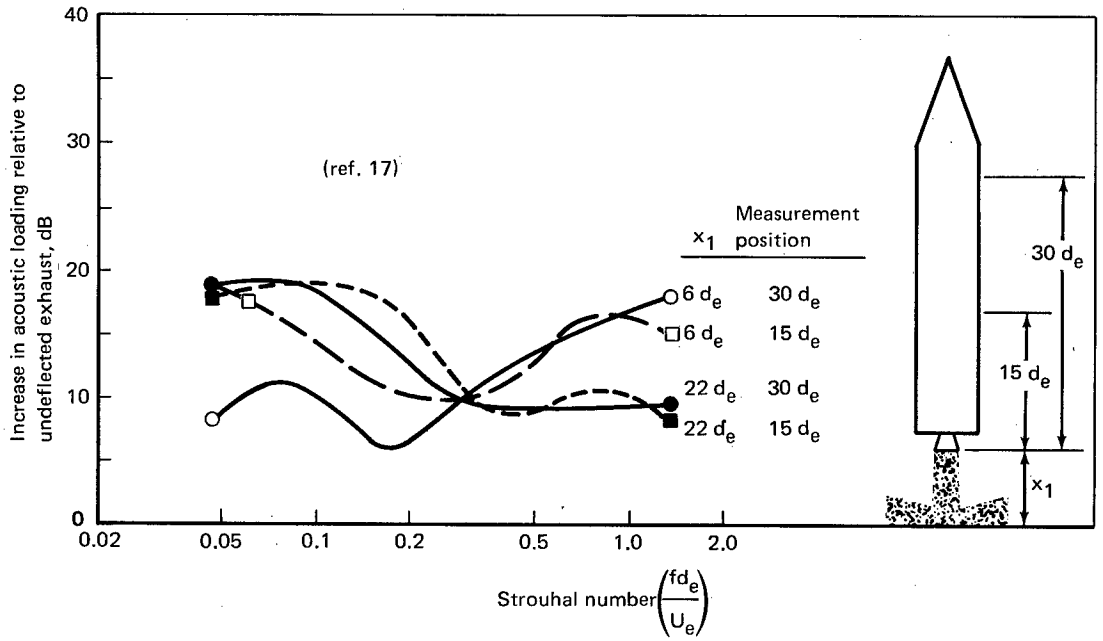

(a) 90-deg flat-plate deflector at two distances (x_1) from nozzle.

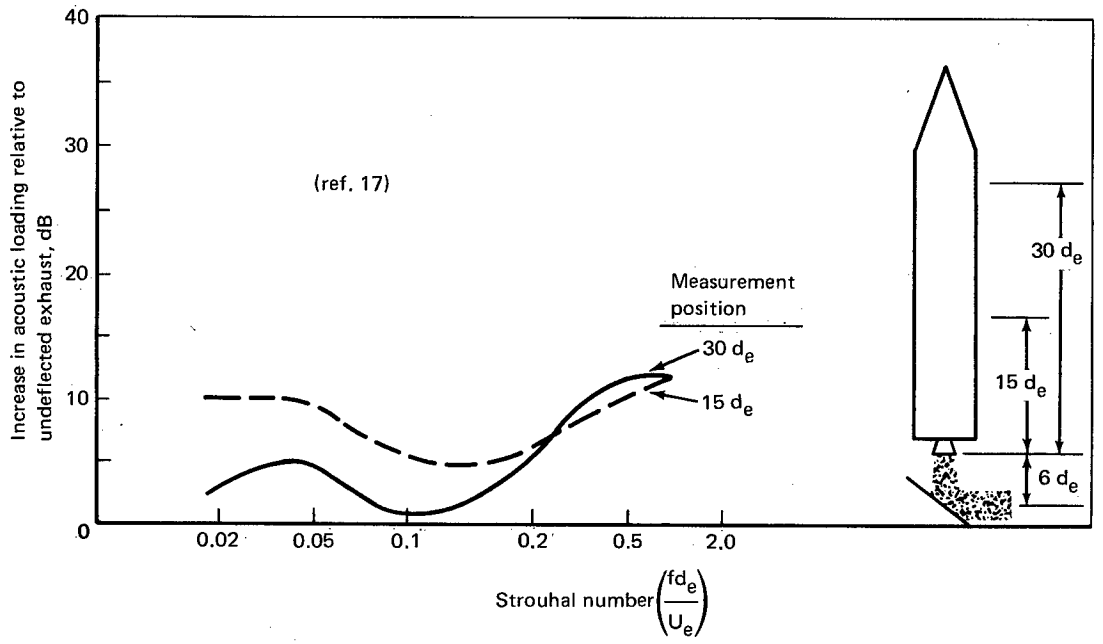

(b) 45-deg flat plate [measured on side of vehicle toward flow (ϕ = 0)]

Figure 15. – Examples of the increase in noise level as a result of deflecting the exhaust flow.

energy transferred from the pressure fluctuations to the structural-response mode. Experimental measurements of correlation patterns along the vehicle are limited to a single known case, and the results are summarized in reference 31. Theoretical

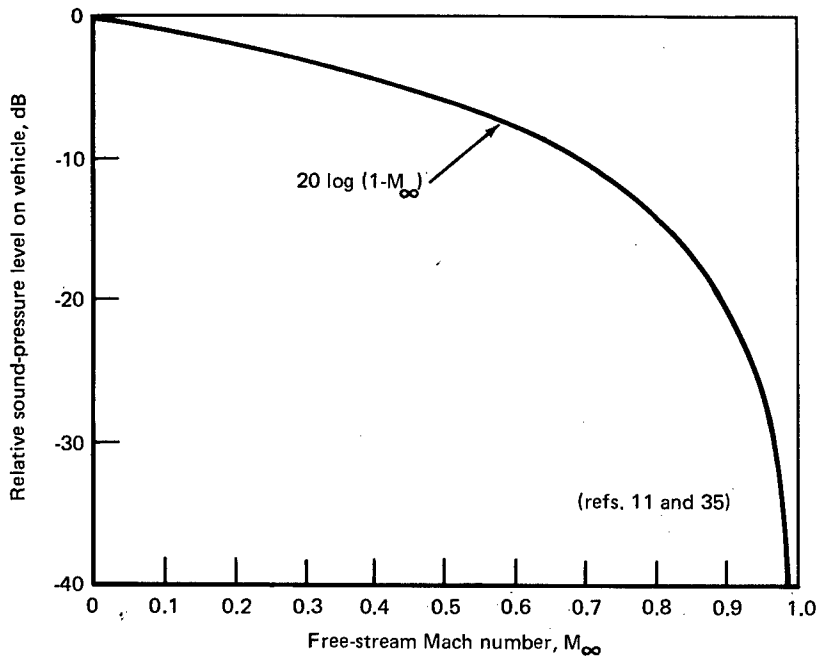

Figure 16. – Estimated effect of vehicle velocity on acoustic loading for undeflected rocket exhaust.

calculations of correlation using a source-distribution technique are reported in reference 34; the computation involves extensive mathematical manipulations to include the scattering from the vehicle. The correlation curves calculated in references 30 and 31 for the geometry of figure 17 are normalized in terms of frequency and principal angle of radiation for that particular frequency, and the results are given for circumferential correlation (fig. 18) and longitudinal correlation (fig. 19).

2.3 Prediction Methods for Near-Field Noise

Near-field noise levels can either be predicted analytically, using normalized results obtained from experimental acoustical measurements, or be measured directly by an acoustical test using either full or subscale models.

2.3.1 Empirical Analysis

The following prediction methods are typical of those which have been used. They are presented in order of increasing complexity.

- Extrapolation of measured data from similar configurations to predict sound-pressure spectra at various positions on the vehicle. Figure 20 (taken from ref. 36) shows some typical results, which are estimated to have an accuracy of ±6 dB for prediction purposes for the configuration noted in the figure.

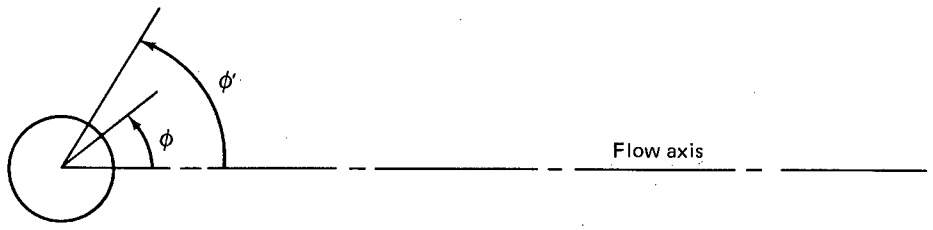

(a) Top view

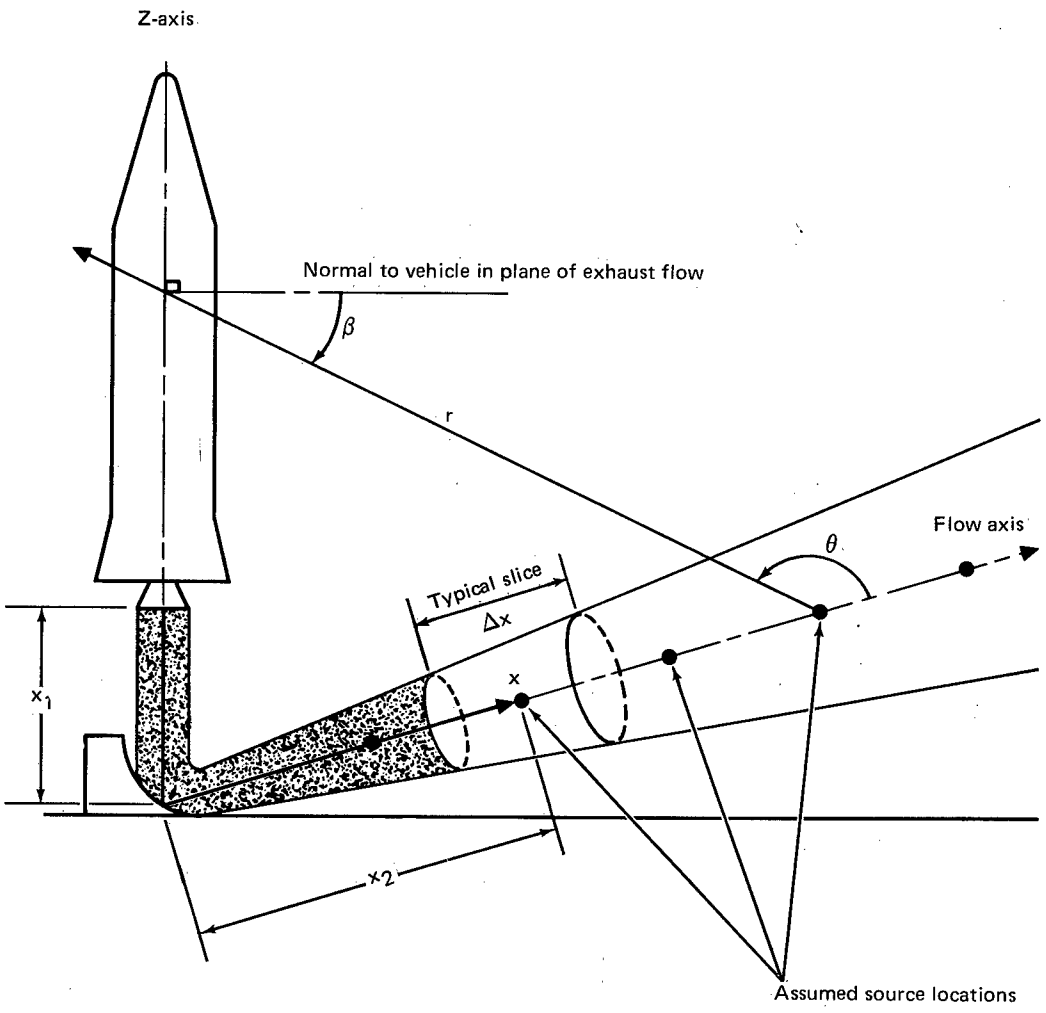

$x = x_1 + x_2$

(b) Side view

Figure 17. – Sketch of source locations and geometry for figures 18 and 19.

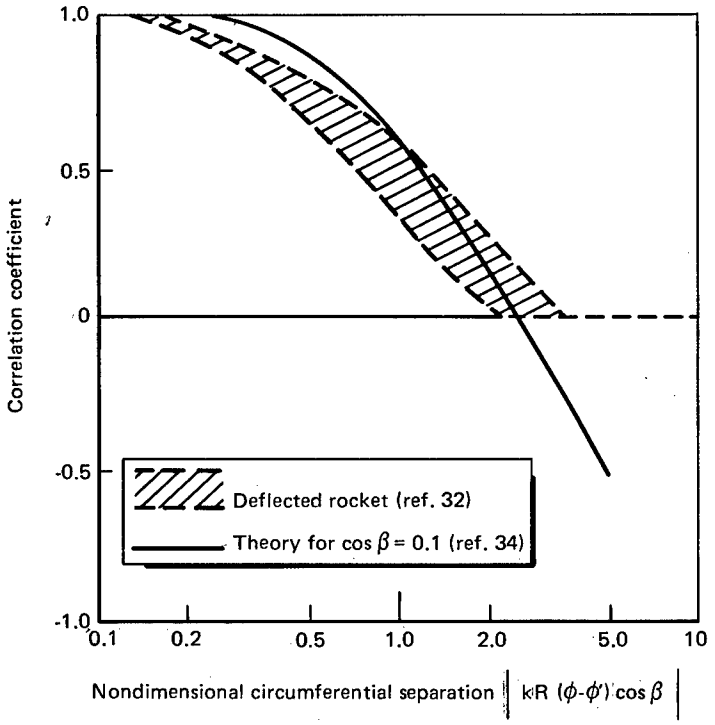

Figure 18. – Circumferential correlation of acoustic pressures for angle ϕ and separation (ϕ-ϕ').

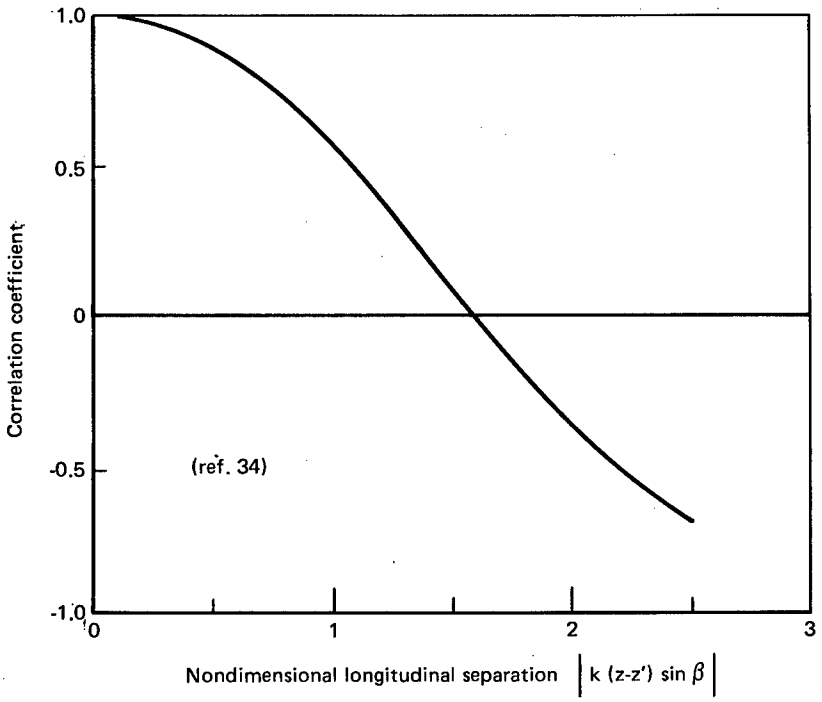

Figure 19. – Longitudinal correlation of acoustic pressures on a space vehicle for position z and vertical separation (z-z').

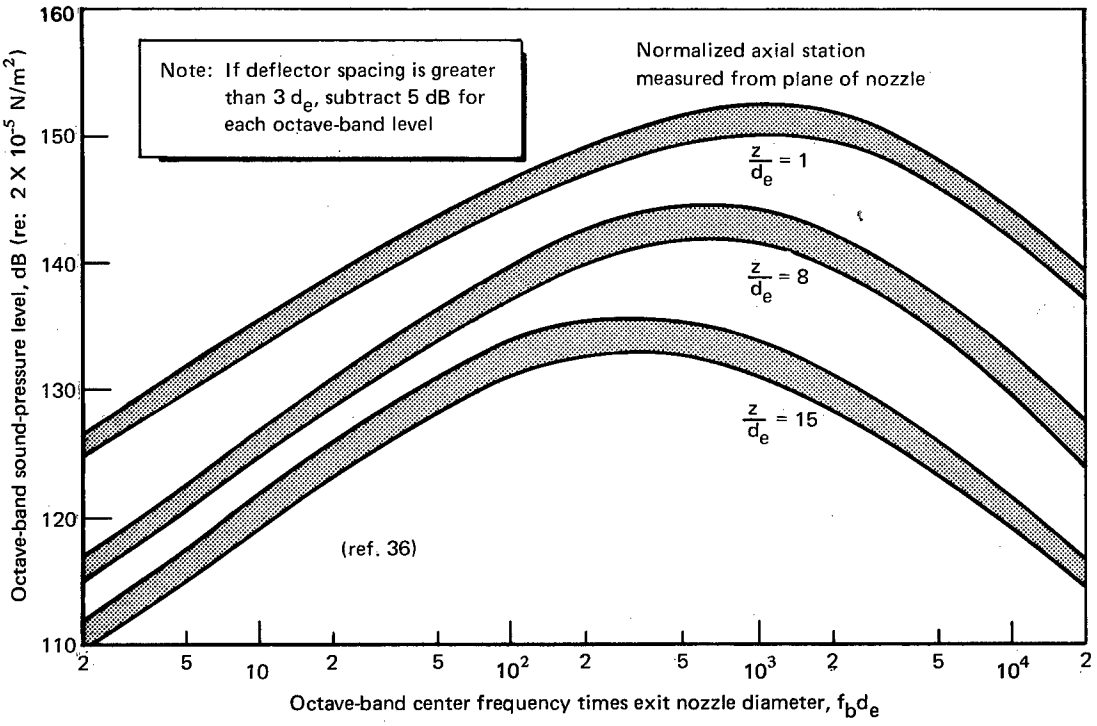

Figure 20. – Sound-pressure levels on space vehicle on launch stand–for simple deflector geometries which change the flow direction approximately 90 degrees from the vehicle axis.

- A source-distribution technique, whereby octave-band or 1/3-octave-band sources are allocated along the deflected exhaust stream. The radiated field from each source is then summed to obtain the loading for the required point on the vehicle. An assumption regarding the directivity is necessary, and far-field results are often used. Such a technique is outlined in reference 31. This technique is estimated to have an accuracy of ±4 dB for prediction purposes for standard configurations, when exhaust shielding and reflections are of little importance.

- A more complex analytic source-distribution technique, involving the allocation of a spectrum of sources at selected points along the flow. Again, addition of the individual fields gives the final loading. This technique (ref. 10) is estimated to have an accuracy of ±4 dB for prediction of standard configurations, and enables a better assessment of the effect of exhaust shielding and reflections on the acoustic levels and spatial correlations.

The effect of reflection and scattering can be included in additional studies, and a final analytic stage involves calculating correlation curves for the spatial-loading pattern on the vehicle. The individual sources are assumed to be completely uncorrelated, so that

the results for each source can be simply added (ref. 34). Alternatively, when little shielding exists, normalized results such as shown in figures 18 and 19 can be read directly. Additional comments and suggestions for prediction techniques can be found in references 37 to 41.

2.3.2 Experimental Determination

Subscaled models are used in a test program to predict the acoustic loading on a vehicle of new design. Such a program attempts to reproduce the exhaust-flow properties for geometrically similar model rocket nozzles. It also includes geometrically similar configuration variables, including nozzles, deflectors, shrouds, reflecting surfaces, vehicle external surface, and atmospheric parameters.

Full-scale testing of engines on a test stand may also be used to estimate vehicle loading or to validate analytical prediction. Here, caution must be exercised in estimating the effects of reflecting surfaces, which either exist in the test configuration but not in the launch configuration, or vice versa.

A quantitative determination of the acoustic loading from properly conducted subscale or full-scale test programs gives a more accurate prediction than that obtained through empirical analysis. This technique is estimated to have a potential accuracy of ±2 dB, and can include all the effects of exhaust shielding, nonstandard geometry, and reflections on the acoustic loading.

2.4 Minimizing the Acoustic Loads

A method used to eliminate problems associated with acoustic loading predicted by preliminary analysis is to reduce the acoustic loads. These loads can be minimized by several techniques.

One of the techniques for suppressing the sound generated is the injection of water into the exhaust stream. A model study (ref. 42) has shown that significant reduction of the generated sound level is attainable by massive injection of water into the deflector to mix with the exhaust stream. However, the results show that very large quantities of water are necessary, and such systems appear impractical for large boosters. For example, to obtain a power decrease of 10 dB, the addition of water equal to twice the mass flow of the exhaust is required. An indication of approximate reductions in power for full-sized rockets is shown for single engines with water-mass-flow ratios of 2 to 3.5 (ref. 43); however, other configuration variables may be responsible. In fact, little effect is noticed for an eight-engine configuration with a mass-flow ratio of 1.

Directing the exhaust gas into a body of water will also reduce the generated noise. Data collected from tests with models (ref. 17) show reduction up to 10 dB initially, although continued engine operation quickly emptied the water tank. A test stand that directed the vehicle's exhaust into a large lake could produce a continuous reduction; however, the engineering problems associated with building such a stand would be formidable.

The maximum reduction in acoustic loading to be sought in ground operation for vehicle-design purposes is on the order of 15 to 20 dB; any further suppression would not be meaningful to vehicle design since the vehicle would ordinarily encounter a higher level of noise during flight.

The acoustic loading on the vehicle can also be reduced by design. Selection of less-noisy rocket engines will not normally be possible since engine selection is determined by other requirements. However, an immediate reduction can be achieved by choosing an engine with a lower exhaust velocity, which in turn is determined by the choice of propellants. Where multiple engines are involved, their location with respect to the vehicle structure can alleviate the noise exposure of that structure. The structure located near the engines will be subjected to similar levels for all configurations, but the choice of layout of the nozzles can affect the spectrum of sound thus formed. A wider spacing can give a broader spectrum, with resulting lower peak levels of sound generation (refs. 20 and 21).

The test and launch stands can be designed to reduce the levels on the vehicle surface. By making sure that the exhaust flow is deflected through a minimum angle, the levels on the vehicle can be substantially reduced. During launch, this reduction can be in the order of 10 dB as indicated in figure 15. In addition, the use of a roof over the deflector to form a tunnel and enclose the sound field can provide further reduction in levels on the vehicle, especially when the vehicle is close to the launch stand. The amount of reduction is totally dependent upon the individual launch-stand design; however, reductions of 20 dB or more can be expected.

The influence of surfaces near the vehicle, which will tend to cause local increases in level, can be minimized by careful design of the support facilities. Alternatively, acoustic blankets designed to attenuate sound can be placed over areas of the vehicle, and attenuations of 5 to 10 dB can be achieved by use of lightweight blankets (author's unpublished work).

3. CRITERIA

Acoustic loads generated by a space vehicle's propulsion system shall be determined by a suitable combination of analysis and test, and the results given in parameters useful

for determination of acoustic loads for structural design. The prediction of acoustic loading that may affect the integrity of the structure shall account for all significant exhaust-flow properties, configuration variables, and parameters of the vehicle and the atmosphere. Tests shall be conducted to verify analysis or, for a significantly different configuration, to determine the acoustic loads. If the predicted acoustic loads adversely affect design, the feasibility of minimizing the loads shall be accurately evaluated.

3.1 Acoustic-Load Parameters

To the extent required for design, the predicted acoustic loads shall be given as a function of position and time in terms of:

- Overall sound-pressure level
- Frequency spectrum
- Spatial correlation

3.2 Prediction of Acoustic Loads by Empirical Analysis

Where the propulsion is provided by a rocket whose design and deflectors are typical of those for which acoustical data exist, an empirical analysis shall be made to predict the acoustic loading. The prediction of the acoustic loads required for design shall account for at least the following factors:

- Exhaust-flow properties
  - (a) Jet-exit velocity
  - (b) Jet-exit density
  - (c) Jet-exit Mach number
  - (d) Jet-exit static pressure
- Configuration variables
  - (a) Nozzle-exit diameter, shape and area ratio
  - (b) Multiple-nozzle geometry
  - (c) Deflector geometry, including distance between nozzle and deflector

(d) Exhaust-shroud geometry

(e) Reflecting-surface geometry

- Vehicle parameters

  (a) Vehicle configuration

  (b) Velocity

- Atmospheric parameters

  (a) Pressure

  (b) Temperature

  (c) Gas composition

3.3 Testing

3.3.1 Subscale Model Tests

Acoustical models shall be tested as necessary during the design process to improve the accuracy of the predicted acoustic loads. Model testing shall also be performed when the test stand, launch system, or vehicle configurations under design differ significantly from those on which data are available. Additionally, unless testing can be demonstrated unnecessary, subscale model testing shall be conducted when any of the following conditions exist:

- Exit-gas velocity is greater than 3000 m/sec
- Exit-gas density is greater than that of the ambient atmosphere, or less than 0.05 kg/m^3
- Nozzle configuration deviates significantly from standard practice
- Nozzle-exit static-pressure ratio is greater than 2
- Deflector and/or shroud design deviates significantly from standard practice
- Atmospheric conditions differ significantly from those existing on the earth's surface

3.3.2 Full-Scale Tests

When the acoustic loading on the vehicle is critical to the design, acoustical measurements shall be made during static-firing tests and launch of test vehicles.

3.4 Minimizing the Acoustic Loads

If, for a given design, the acoustic loading from the propulsion system results in a significant problem, tradeoff studies shall be made to determine the feasibility of minimizing the acoustic loading through noise reduction, flow control, or shielding techniques without unduly affecting vehicle performance or integrity.

4. RECOMMENDED PRACTICES

In determining space vehicle acoustic loads generated by its propulsion system, it is recommended that initial analysis and/or test predictions be made and the results studied to determine whether additional analysis and/or tests are needed to obtain more accurate acoustic loadings. Empirical-analysis methods such as those recommended in Section 4.2 are suitable for initial prediction of the acoustic loads on space vehicles, particularly for vehicles with chemical rockets whose nozzle design and exhaust-flow characteristics are typical of current propulsion systems. For such typical propulsion systems, these methods are considered adequate for providing inputs to preliminary design-tradeoff studies for optimization of the configuration, estimating the vibration environment, and determining the degree of criticality of the acoustic load on the structure. The results obtained using these methods should be supplemented by any available additional data pertaining to similar vehicle configurations.

When the results of these analyses and any available data from similar vehicles indicate that acoustic loads are critical for part of the vehicle structure, or when new designs and configurations are proposed for the space vehicle which differ significantly from existing rockets as detailed in Section 3.3.1, test programs such as recommended in Section 4.3 are necessary to predict the acoustic loading. When the results of the foregoing analysis and/or tests indicate potential problems resulting from the predicted acoustic loading, methods for minimizing the acoustic loading, such as recommended in Section 4.4, should be considered.

4.1 Acoustic-Load Parameters

It is recommended that analysis, test procedures, and test instrumentation be carefully planned so that the results yield data from which the acoustic loads can be formulated in terms of the parameters given in the criteria of Section 3.1.

4.2 Prediction of Acoustic Loads by Empirical Analysis

Three prediction methods were discussed in Section 2.3.1. The first method estimates the octave-band noise levels over the vehicle by direct use of figure 20. This method may be useful for preliminary rough estimates, but it is not recommended for a formal preliminary loads definition.

The recommended methods for predicting acoustic loads are the two source-allocation methods based on allocating the noise-generation sources along the exhaust stream (refs. 10, 31, 34, and 37). The following summarizes the detailed steps for prediction of the overall-sound-pressure-level spectrum at a point, p, on the vehicle (not including effects of reflecting surfaces). The first source-allocation method uses the technique of assigning each frequency band a unique source location along the flow axis as follows:

1. Determine the flow axis relative to the vehicle and the stand. (Note that distance, x, along the flow axis is measured from the nozzle, as illustrated in fig. 17).

2. Estimate the overall acoustic power from:

$$W_{OA} = 0.005\ n\ FU_e \tag{1}$$

where

W_{OA} = overall acoustic power, W

F = thrust of each engine, N

n = number of nozzles

U_e = fully expanded exit velocity, m/sec

(Note that this equation conservatively assumes the efficiency of noise generation to be one percent).

3. Calculate the overall sound power level, L_W from:

$$L_W = 10 \log W_{OA} + 120, \text{ dB (re } 10^{-12} \text{ watts)}. \tag{2}$$

4. If the vehicle has more than one nozzle, compute an exit-nozzle diameter for use in the figure from:

$$d_e = \sqrt{n}\, d_{ei} \tag{3}$$

where d_{ei} = the exit diameter of the individual nozzle.

5. Convert the normalized spectrum of figure 5 to a conventional acoustic bandwidth (i.e., the power spectrum per Hz, per 1/3 octave, or per octave, as desired) from:

$$L_{w,b} = 10 \log \left[\frac{W(f)}{W_{OA}} \frac{U_e}{d_e} \right] + L_w - 10 \log \frac{U_e}{d_e} + 10 \log \Delta f_b \qquad (4)$$

where

$L_{w,b}$ = sound-power level in the band centered on frequency b, dB (re 10^{-12} W)

Δf_b = bandwidth of the frequency band, Hz.

6. Allocate the acoustic sources along the exhaust-flow center line. The location of a single source for each frequency band, either 1/3 octave or octave band, is determined by arranging a source of strength given by the acoustic-power spectrum at points given by the solid-line curve of figure 14. This line (ref. 31) is the preferred curve, although the result should be modified according to the broken line if a closed-bucket-type deflector is used.

7. Calculate the sound-pressure level in the band centered on any frequency, b, and at any point, p, on the vehicle from:

$$SPL_{b,p} = L_{w,b} - 10 \log r^2 - 11 + DI(b,\Theta) \qquad (5)$$

where

$SPL_{b,p}$ = sound-pressure level at position p, in the band centered on frequency b, dB (re 2×10^{-5} N/m^2).

r = length of the radius line from the assumed position of the frequency source to the point on the vehicle (see fig. 17), m

Θ = angle between the flow centerline and r (see fig. 17)

$DI(b,\Theta)$ = directivity at the angle Θ for the band centered on frequency b (see fig. 10), dB.

8. Calculate the overall sound pressure level at any point, p, on the vehicle by logarithmic summation of $SPL_{b,p}$ over the entire spectrum from:

$$SPL_{OA,p} = 10 \log \sum_{\text{All b}} \left[\text{antilog} \frac{SPL_{b,p}}{10} \right], \text{ dB (re } 0.2 \times 10^{-5} \text{ N/m}^2). \qquad (6)$$

The second source-allocation method recognizes that the noise in each frequency band is generated throughout the flow, rather than at a discrete location as assumed above. This method is more difficult to apply than that using the discrete model but is necessary when an acoustical shielding between the flow and the vehicle must be accounted for. The steps are as follows:

1 through 4. (See first method presented earlier in this section.)

5. Determine the length of the core, x_t, from figure 11.

6. Divide the rocket flow into a number of slices as illustrated in figure 17.

7. Obtain the normalized acoustic power per unit core length $10 \log [x_t W(x)/W_{OA}]$ from figure 12.

8. Calculate the overall acoustic power for each slice, $L_{W,S}$, from:

$$L_{W,S} = 10 \log \left[\frac{x_t W(x)}{W_{OA}} \right] + L_W + 10 \log \frac{\Delta x}{x_t}, \text{ dB (re } 10^{-12} \text{ W)} \qquad (7)$$

where Δx = length of the slice.

9. Convert the normalized spectrum of figure 13 to a conventional acoustic bandwidth (i.e., the power spectrum per Hz, per 1/3 octave, or per octave, as desired) for each slice, using:

$$L_{W,S,b} = 10 \log \left[\frac{W(f,x)}{W(x)} \frac{U_e a_o}{x a_e} \right] + L_{WS} - 10 \log \frac{U_e a_o}{x a_e}$$

$$+ \log \Delta f_b, \text{ dB (re } 10^{-12} \text{ watts)} \qquad (8)$$

where

$W(f,x)$ = sound power per Hz per unit axial length at distance x along the flow axis, W/Hz/m

x = distance along the flow axis from the nozzle to the center of the slice, m

a_o = speed of sound in the atmosphere, m/sec

a_e = speed of sound in the flow at the nozzle exit, m/sec

10. Compute the sound pressure level in each frequency band at each point contributed by each slice, $SPL_{s,b,p}$, from:

$$SPL_{s,b,p} = L_{w,s,b} - 10 \log r^2 - 11 + DI\,(b,\Theta) \tag{9}$$

(Note: $SPL_{s,b,p}$ may be altered as required to account for reflections).

11. Compute the sound-pressure level in each frequency band at each point by logarithmic summation of contributions from each of the slices from:

$$SPL_{b,p} = 10 \log \sum_{s} \text{antilog} \frac{SPL_{s,b,p}}{10} \tag{10}$$

where $SPL_{b,p}$ = total SPL in the frequency band b at the point, p, dB (re 2×10^{-5} N/m^2)

12. Using equation (6), calculate the overall sound pressure at any point, p, by logarithmic summation of $SPL_{b,p}$.

On the surface of the vehicle, immediately facing the exhaust flow, the pressure will increase over that predicted in the free-field because of the reflection of the sound at the surface. This will cause a local increase in sound-pressure level of as much as 6 dB, depending on the angle of incidence. At the sides of the vehicle, the levels will be as predicted for the free field; opposite from the flow, the shielding of the vehicle will reduce the level. This effect will be complicated for a configuration with twin exhaust flows such as produced by a double deflector. In this case, the individual flows should be treated in turn. Considering the scattering, as from an infinite cylinder, permits an exact calculation of the pressure field on the vehicle; typical values and results for a large first-stage booster are given in reference 34.

The effect of large reflecting surfaces such as launch-stand walls should be included in the prediction by estimating the additional noise contributed to the point under consideration. Levels on the vehicle will be increased 3 to 6 dB, as shown in references 9 and 13, when a reflected field also loads the point under consideration. If the geometry of the reflecting structure is complex, then the use of experimental measurements, either subscale or full scale, is essential for accurate prediction.

Spatial correlation may be estimated with the normalized curves of figures 18 and 19, which are based on references 31 and 34. To use these results, a location of maximum

source strength for each frequency is determined as done in the first source-allocation method, and the angle, β, determined by constructing the line from this point to the position under consideration, as illustrated in figure 17. A more detailed estimate of the spatial correlation may be obtained by computing the correlation for $SPL_{s,b,p}$, using figures 18 and 19 as before, but computing β for each slice. This more detailed estimate accounts approximately for the angular distribution of the sound incident on the surface and can be used to estimate the structural response to the noise from each slice of the noise flow, summing the responses on an energy basis in each frequency band. If subsequent calculation suggests that the structural loading could be critical, then experimental measurement of the correlation pattern is desirable.

A final calculation should be completed to examine the effects of the initial liftoff period. Following the foregoing procedure, the designer should consider the vehicle to be in an elevated position and then examine the levels resulting from the new source distribution. Because the low-frequency acoustic sources may be nearer to the vehicle, the critical point will be to determine if there is any increased low-frequency loading.

4.3 Testing

The prediction of acoustic-pressure levels for unusual stand and deflector configurations and for new engines with different exhaust-flow properties will require the use of experimental measurements. These measurements can be obtained with either a subscale or a full-scale experiment.

4.3.1 Subscale Model Tests

Model tests are based on a geometrically scaled model of the propulsion nozzles, vehicle, deflector, and stand. When model tests are necessary, the degree of simulation required is dependent upon the information required for acoustic-load definition. However, in all cases it is essential that the rocket-exhaust gas-flow properties be properly simulated. The exhaust-gas density, velocity, Mach number, and exit static pressure should be the same as full scale, which means that the use of model rockets is preferred. Substitute gases may be used, and heated helium (ref. 13) has proven to be the most useful (heated air jets are not suitable). The model nozzles should be scaled from the full-scale engine with the correct exit area and expansion ratio. It is recommended that multinozzle arrangements be similarly scaled, but they may be attached to a single combustion chamber (ref. 20).

In general, accuracies of a few percentages are adequate for geometric scaling of configuration variables, although the model nozzles are often fabricated with much higher accuracy. The effect of inaccuracies on exhaust-flow parameters may be estimated from figures 3 and 5, and additionally from data in references 10 and 12.

Usually, an accuracy of approximately 5 percent in flow parameters should be satisfactory. Measurement of velocity and temperature are recommended, where practical, in addition to measurement of chamber pressure; shadowgraph photographs are useful to determine the geometry of the exhaust plume through the deflector.

The choice of a geometric scale factor must be carefully considered. Model nozzle throats of 0.013-m (1/2-in.) diameter have been used with apparent success. But caution must be exercised in the choice of significantly smaller nozzles because of the possibility of boundary-layer effects associated with low Reynolds numbers. The frequency region of principal interest for acoustic loading must also be considered. Microphones can be obtained that are capable of good response to 100 000 Hz, but if they are to be used for spatial-correlation measurements of sound that is parallel to a surface, their diameter should be less than 1/8 of the acoustic wavelength at the highest frequency of interest. Because of these problems, the largest practicable models are generally used, with a geometric scale factor not smaller than 1/20.

Accurate calibration of the instrumentation system over the entire frequency range is necessary (e.g., refs. 44 to 46). Also, when correlation measurements are being taken, there is little tolerance for interchannel-phase shift and direct digital recording is preferable. A useful final check for a model program is to conduct a complete far-field survey at a radius of approximately $100\,d_e$, then to compare the data to the generalized results of figures 3 and 5 to note anomalies in the model and instrumentation systems.

4.3.2 Full-Scale Tests

Full-scale measurements of the vehicle's acoustic loads should be obtained if feasible during the development of the engines. Deflectors on the engine test stands should be similar to deflectors used at the launch stand. Then, after erecting surfaces to represent major reflecting surfaces of the proposed stand and other structures to simulate the vehicle, it is possible to obtain representative measurements of the acoustic field over the proposed vehicle.

Similarly, measurement of the acoustic pressure at a minimum of one significant point on the vehicle should be made early in the test-stand firing phase of the vehicle to verify the predicted levels.

Data should be obtained over a frequency range of approximately 20 to 10 000 Hz. Calibration precautions should be observed, as discussed in the previous section. Microphone location will depend upon vehicle configuration and predicted regions of difficulties resulting from acoustic loading. Correlation measurements should be made over typical simulated skin panels predicted to be critical. Such measurements should

include at least one vertical and one circumferential microphone array or traverse. For fixed arrays, primary emphasis in selection of microphone spacing should be placed in the frequency region of critical interest for panel response.

4.4 Minimizing the Acoustic Loads

When, as specified in the criteria, it is necessary to make tradeoff studies to consider the feasibility of minimizing the acoustic loads, it is recommended that such studies be made in the vehicle design stage. The recommended methods for minimizing the acoustic loads are the noise reduction, flow control, and shielding techniques as described in Section 2.4. A minimum acoustic loading will result when:

- The angle through which the exhaust flow is deflected is kept as small as possible. This will normally require the vehicle to be set at some distance above the ground; otherwise, a deflection angle of greater than 90 degrees will result with increased acoustic levels.

- The exhaust flow is deflected through a covered bucket or tunnel to shield the vehicle from direct radiation from the deflected flow.

- The deflector and test stand are designed to eliminate large reflective surfaces turned toward the space vehicle.

- Water is injected into the deflector near the nozzle.

- Acoustical-attenuation padding is placed over sensitive areas of the vehicle.

APPENDIX

DEFINITIONS OF ACOUSTICAL TERMINOLOGY

Acoustic Loading—Acoustic loading is the spatially- and frequency-dependent sound-pressure fluctuations on the vehicle surface.

Decibel (p. 13, ref. 47)—The decibel is a unit of level when the base of the logarithm is the tenth root of ten, and the quantities concerned are proportional to power.

Note 1: Examples of quantities that qualify are power (any form), sound-pressure squared, particle-velocity squared, sound intensity, sound-energy density, voltage squared. Thus the decibel is a unit of sound-pressure-squared level; it is common practice, however, to shorten this to sound-pressure level because ordinarily no ambiguity results from so doing.

Note 2: The logarithm to the base the tenth root of 10 is the same as ten times the logarithm to the base 10; e.g., for a number X^2, $\log_{10^{1/10}} X^2 = 10 \log_{10} X^2 = 20 \log_{10} X$. This last relationship is the one ordinarily used to simplify the language in definitions of sound-pressure level, et cetera.

Directivity Factor (p. 20, ref. 47)—(1) The directivity factor of a transducer used for sound emission is the ratio of the sound pressure squared, at some fixed distance and specified direction, to the mean-square sound pressure at the same distance averaged over all directions from the transducer. The distance must be great enough so that the sound appears to diverge spherically from the effective acoustic center of the sources. Unless otherwise specified, the reference direction is understood to be that of maximum response.

(2) The directivity factor of a transducer used for sound reception is the ratio of the square of the open-circuit voltage produced in response to sound waves arriving in a specified direction to the mean-square voltage that would be produced in a perfectly diffused sound field of the same frequency and mean-square sound pressure.

Note 1: This definition may be extended to cover the case of finite frequency bands whose spectrum may be specified.

Note 2: The average free-field response may be obtained in various ways, such as:

(a) By the use of a spherical integrator

(b) By numerical integration of a sufficient number of directivity patterns corresponding to different planes

(c) By integration of one or two directional patterns whenever the pattern of the transducer is known to possess adequate symmetry.

Directivity Index (p. 30, ref. 47)—The directional gain of a transducer, in decibels, is 10 times the logarithm to the base 10 of the directivity factor.

Level (p. 13, ref. 47)—In acoustics, the level of a quantity is the logarithm of the ratio of that quantity to a reference quantity of the same kind. The base of the logarithm, the reference quantity, and the kind of level must be specified.

Note 1: Examples of kinds of levels in common usage are electric power level, sound-pressure-squared level, voltage-squared level.

Note 2: The level as here defined is measured in units of the logarithm of a reference ratio that is equal to the base of logarithms.

Note 3: In symbols,

$$L = \log_r (q/q_0)$$

where

L = level of kind determined by the kind of quantity under consideration, measured in units of $\log_r r$

q = the quantity under consideration

q_0 = reference quantity of the same kind

r = base of logarithms and the reference ratio

Note 4: Differences in the levels of two like quantities q_1 and q_2 are described by the same formula because, by the rules of logarithms, the reference quantity is automatically divided out:

$$\log_r (q_1/q_0) - \log_r (q_2/q_0) = \log_r (q_1/q_2)$$

Overall Sound-Pressure Level—The overall sound-pressure level is the sound-pressure level over all frequencies in the frequency range of interest, usually 22.5 - 11 200 Hz for full-scale vehicles.

Power Level (p. 14, ref. 47)—Power level, in decibels, is 10 times the logarithm to the base 10 of the ratio of a given power to a reference power. The reference power must be indicated.

Note: In sound recording, for example, a reference electric power often used is the milliwatt, and the symbol dbm is employed to indicate both the unit of power level, the decibel, and the reference power, the milliwatt.

Power Spectrum (p. 11, ref. 47)—The spectrum density of an oscillation is the mean-square amplitude of the output of an ideal filter with unity gain responding to the oscillation, per unit bandwidth; i.e., the limit for vanishingly small bandwidth of the quotient of the mean-square amplitude divided by the bandwidth.

Note 1: In mathematical terms, the spectrum density function of an oscillation y(t) is the ensemble average of G(f) where (when a limit exists)

$$G(f) = \lim_{T \to \infty} \frac{1}{T} \left| \int_{-T}^{T} y(t)\, e^{2\pi i f t}\, dt \right|^2$$

f being frequency (positive only).

Note 2: The mean-square output of an ideal filter with unity gain in a finite band is given by the integral of G(f) with respect to frequency over the band.

Sound Power (p. 13, ref. 47)—The sound power of a source is the total sound energy radiated by the source per unit of time.

APPENDIX

Sound Pressure (p. 12, ref. 47)—The sound pressure at a point is the total instantaneous pressure at that point in the presence of a sound wave minus the static pressure at that point.

Sound Pressure Level (p. 14, ref. 47)—The sound pressure level, in decibels, of a sound is 20 times the logarithm to the base 10 of the ratio of the pressure of this sound to the reference pressure. The reference pressure shall be explicitly stated.

Note 1: The following reference pressures are in common use:

(a) 2×10^{-4} microbar

(b) 1 microbar

Reference pressure (a) is in general use for measurements concerned with hearing and with sound in air and liquids, while (b) has gained widespread acceptance for calibration of transducers and various kinds of sound measurements in liquids.

Note 2: Unless otherwise explicitly stated, it is to be understood that the sound pressure is the effective (rms) sound pressure.

Note 3: It is to be noted that in many sound fields the sound-pressure ratios are not the square roots of the corresponding power ratios.

Spatial Correlation—Spatial correlation is a measure of the distance in a given direction over which the sound pressure in a stated frequency band may be considered in phase. The sound at two points (1 and 2) is said to be fully correlated when the pressure fluctuations (p_1 and p_2) are in phase; i.e., when

$$\frac{\overline{p_1\, p_2}}{(\overline{p_1^2})^{1/2}\,(\overline{p_2^2})^{1/2}} = 1$$

Spectrum (p. 11, ref. 47)—(1) The spectrum of a function of time is a description of its resolution into components, each of different frequency and (usually) different amplitude and phase.

(2) "Spectrum" is also used to signify a continuous range of components, usually wide in extent, within which waves have some specified common characteristic; e.g., "audio-frequency spectrum." (Note: The term "spectrum" is also applied to functions of variables other than time, such as distance.)

REFERENCES

1. Anon.: Structural Vibration Prediction. NASA Space Vehicle Design Criteria (Structures), NASA SP-8050, 1970.

2. Anon.: Buffeting During Atmospheric Ascent. NASA Space Vehicle Design Criteria (Structures), NASA SP-8001, revised 1970.

3. Lighthill, M. J.: On Sound Generated Aerodynamically, I, General Theory. Proc. Roy. Soc. (London), A211, 1952, pp. 564-587.

4. Lighthill, M. J.: On Sound Generated Aerodynamically, II, Turbulence As a Source of Sound. Proc. Roy. Soc. (London), A222, 1954, pp. 1-32.

5. Ffowcs-Williams, J. E.: The Noise from Turbulence Convected at High Speed. Phil. Trans. Roy. Soc. (London), A255, 1963, pp. 469-503.

6. Lighthill, M. J.: The Bakerian Lecture, 1961, Sound Generated Aerodynamically. Proc. Roy. Soc. (London), A267, 1962, pp. 147-182.

7. Lighthill, M. J.: Jet Noise. AIAA J., vol. 1, no. 7, July 1963, pp. 1507-17.

8. Ribner, H. A.: The Generation of Sound by Turbulent Jets. Advances in Applied Mechanics, H. L. Dryden and Th. von Karman., eds. Vol. VIII, Academic Press, (New York), 1964, pp. 103-182.

9. Eldred, K. McK.; Mann, M.; White, R. W.; and Cottis, M.: Suppression of Jet Noise with Emphasis on the Near Field. ASD-TDR-62-578, Wright Patterson AFB, Ohio, Feb.1963.

10. Potter, R. C.; and Crocker, M. J.: Acoustic Prediction Methods for Rocket Engines, Including the Effects of Clustered Engines and Deflected Exhaust Flow. NASA CR-566, 1966.

11. Eldred, K. McK.; Roberts, W.; and White, R. W.: Structural Vibrations in Space Vehicles. WADD TR 61-62, Mar. 1961.

12. Morgan, W. V.; Sutherland, L. C.; and Young, K. J.: The Use of Acoustic Scale Models for Investigating Near Field Noise of Jet and Rocket Engines. WADD TR 61-178, Apr. 1961.

13. Morgan, W. V.; and Young, K. J.: Studies of Rocket Noise Simulation with Substitute Gas Jets and the Effect of Vehicle Motion on Jet Noise. ASD-TDR-62-787, Wright-Patterson AFB, Ohio, Mar. 1963.

14. Gray, C. L.: Study in the Use of Structural Models for Sonic Fatigue. ASD TR-61-547, Apr. 1962. (Available from DDC as AD 277186.)

15. Cole, J. N.; Von Gierke, H. E.; Kyrasis, D. T.; Eldred, K. McK.; and Humphrey, A. J.: Noise Radiation from Fourteen Types of Rockets in the 1,000 to 130,000 Pound Thrust Range. WADC TR 57-354, 1957.

16. Mayes, W. H.; Lanford, W. E.; and Hubbard, H. H.: Near Field and Far Field Noise Surveys of Solid Fuel Rocket Engines for a Range of Nozzle Exit Pressures. NASA TN D-21, 1959.

17. Cole, J. N.; England, R. T.; and Powell, R. G.: Effects of Various Exhaust Blast Deflectors on the Acoustic Noise Characteristics of 1000 Pound Thrust Rockets. WADD TR 60-6, Sept.1960. (Available from DDC as AD 251833)

18. Kennedy, B.; and Johnson, D. G.: Acoustic Environments of Very Large Solid Propellant Motors. Rept. 219, Datacraft, Inc., Gardena, Calif., 1967.

19. Lassiter, L. W.; and Heitkotter, R. H.: Some Measurements of Noise from Three Solid-Fuel Rocket Engines. NASA TN-3316, 1954.

20. Wiley, D. R.: Clustered Model Rocket Acoustics Test. Rept. T2-2574, The Boeing Co., Mar. 1964. (Available from DDC as AD 448818)

21. Smith, E. G.; and Brown, W. L.: Acoustic Scale-Model Tests of High-Speed Flows, Phase II Final Report. Rept. CR-66-75, Martin Marietta Corp., 1966.

22. Guest, S. H.: Acoustic Efficiency Trends for High Thrust Boosters. NASA TN D-1999, 1964.

23. Manhart, J. K.; Ailman, C. M.; Lane, S. R.; and Marsh, A. H.: An Acoustical Study of the Kiwi B Nuclear Rocket. NASA CR-370, 1966.

24. Tedrick, R. N.: Acoustical Measurements of Static Tests of Clustered and Single-Nozzled Rocket Engines. J. Acoust. Soc. Am., vol. 36, no. 11, Nov. 1964, p. 2027-2032.

25. Atvars, J.; Schubert, L. K.; Grande, E.; and Ribner, H. S.: Refraction of Sound by Jet Flow and Jet Temperature. NASA CR-494, 1966.

26. Grande, E.: Refraction of Sound by Jet Flow and Jet Temperature II. NASA CR-840, 1967.

27. Humphrey, A. J.: Rocket Noise Environments. The Shock and Vibration Bull., No. 25, Part II, Dec. 1957, pp. 10-17.

28. Anderson, A. R.; and Johns, F. R.: Characteristics of Free Supersonic Jet Exhausting into Quiescent Air. Jet Propulsion, vol. 25, no. 1, Jan. 1955, pp. 13-15, 25.

29. Potter, R. C.: An Investigation to Locate the Acoustic Sources in a High Speed Jet Exhaust Stream. Rept. WR 68-4, Wyle Labs., Contract NAS8-21060, NASA CR-101105, 1968.

30. Davies, P. O. A. L.; Fisher, M. J.; and Barratt, M. J.: The Characteristics of the Turbulence in the Mixing Region of a Round Jet. J. Fluid Mech., vol. 15, no. 3, 1963, pp. 337-367.

31. Franken, P.A.; and Staff of Bolt Beranek and Newman: Methods of Space Vehicle Noise Prediction. WADC Tech. Rept. 58-343, Vol. II, Sept. 1960. (Available from DDC as AD 260955)

32. Bollinger, L. E.; Fishbourne, E. S.; and Eske, R.: Contribution of Combustion Noise to Overall Rocket Exhaust Jet Noise. NASA CR-463, 1966.

33. Morse, P. M.: Vibration and Sound. 2nd edition, McGraw-Hill Book Company, Inc., 1948.

34. Potter, R. C.: Correlation Patterns of the Acoustic Pressure Fluctuations on the S-IC Vehicle Due to the Exhaust Noise of the Test and Launch Stand. Rept. WR 66-15, Wyle Labs., Contract NAS8-20073-1, 1966.

35. Powell, A.: On the Effect of Missile Motion on Rocket Noise. J. Acoust. Soc. Am., vol. 30, no. 11, Nov. 1958, p. 1048.

36. Franken, P. A.; and Wiener, F. M.: Estimation of Noise Levels at the Surface of a Rocket-Powered Vehicle. The Shock and Vibration Bull., No. 31, Part 3, Apr. 1963.

37. Franken, P.A.; and Staff of Bolt Beranek and Newman: Methods of Flight Vehicle Noise Prediction. WADC Tech. Rept. 58-343, Nov. 1958. (Available from DDC as AD 205776.)

38. Bond, D. A.: A Summary of Model and Full-Scale Acoustic Data for Prediction of Missile Lift-Off Noise Environments. Rept. NOR-64-215, Northrop Corp., Sept. 1964.

39. Wilhold, G. A.; Guest, S. H.; and Jones, J. H.: A Technique for Predicting Far-Field Acoustic Environments Due to a Moving Rocket Sound Source. NASA TN D-1832, 1963.

40. Peverly, R. W.; and Smith, E. B.: A Practical Method of Predicting the Acoustical Dynamic Environment for Large Booster Launch Facilities. The Shock and Vibration Bull., No. 33, Part II, Feb. 1964.

41. Bies, D. A.; and Franken, P. A.: Notes on Scaling Jet and Rocket Noise. J. Acoust. Soc. Am., vol. 33, no. 9, Sept. 1961, pp. 1171-1173.

42. Shulman, A. L.: Acoustic Evaluation of Water-Cooled Flame Bucket. Rept. AE 61-1140, General Dynamics-Astronautics, Nov. 1961.

43. Dorland, W. D.: Far-Field Noise Characteristics of Saturn Static Tests. NASA TN D-611, 1961.

44. Anon.: Amer. Natl. Stds. Inst. Methods for the Calibration of Microphones. Rept. S1.10-1966, 1966.

45. Anon.: Amer. Nat'l Std. Inst. Method for the Phyical Measurement of Sound. Rept. S1.2-1962, 1962.

46. Anon.: Measurement of Aircraft Exterior Noise in the Field. Rept. ARP 796, SAE, 1965.

47. Anon.: Amer. Nat'l. Std. Inst. Acoustical Terminology. Rept. S1.1-1960, 1960.

SYMBOLS

a	velocity of sound, m/sec
DI	directivity index
d	nozzle diameter, m
F	thrust, N
f	frequency, Hz
k	wave number ($2 \pi f/a$)
L_W	sound-power level, dB (re 10^{-12} W)
$L_{W,b}$	sound-power level in a frequency band centered at frequency b, dB (re 10^{-12} W)
$L_{W,s}$	sound-power level in a slice of the rocket-exhaust flow, dB (re 10^{-12} W)
$L_{W,s,b}$	sound-power level in a slice of the rocket-exhaust flow attributed to frequencies in a frequency band centered at frequency b, dB (re 10^{-12} W)
M	Mach number
n	number of nozzles
R	vehicle radius, m
r	length of the radius line from the assumed position of the frequency source to the point on the vehicle (see fig. 17), m
SPL	sound-pressure level, dB (re 2×10^{-5} N/m^2)
$SPL_{b,p}$	total sound-pressure level in the frequency band b at the point p, dB (re 2×10^{-5} N/m^2)

$SPL_{s,b,p}$	sound-pressure level in frequency band b, at point p contributed by each slice of the rocket-exhaust flow, dB (re 2 x 10^{-5} N/m^2)
SPL(f)	sound-pressure level per Hz, dB (re 2 x 10^{-5} N/m^2)/Hz
U	velocity, m/sec
W	sound power, W
W_{OA}	overall sound power, W
W(f)	sound power per Hz, W/Hz
W(x)	sound power per unit axial length at distance x along flow axis, W/m
W(f,x)	sound power per Hz per unit axial length at distance x along flow axis, W/Hz/m
x	distance from nozzle along flow axis, m
ΔX	length of flow slice, m
z	distance along vehicle axis (in vehicle coordinate system) to point p, m
$z-z'$	distance between points p (coordinates z, ϕ) and p′ (coordinates z′, ϕ), m
β	angle between a line normal to the vehicle axis at point p and the direction line between the apparent source and point p, measured in the plane containing the flow and vehicle axes (see fig. 17), rad
η	acoustic efficiency (rocket-exhaust sound power/rocket-exhaust mechanical power)
θ	angle from exhaust-flow axis (see fig. 17), rad
ϕ	angle around the vehicle, measured from the plane containing the flow and vehicle axes, to a point p (coordinates z, θ) on the vehicle (see fig. 17), rad
$\phi-\phi'$	angle between planes containing points p (coordinates z, ϕ) and p′ (coordinates z, ϕ'), rad

Subscripts:

b	center frequency of band
e	exit (fully expanded)
i	individual nozzle
OA	overall
o	ambient
p	point on vehicle
s	slice
t	tip of supersonic core
u	undeflected
w	power
x	axial distance
∞	free stream

NASA SPACE VEHICLE DESIGN CRITERIA MONOGRAPHS ISSUED TO DATE

SP-8001	(Structures)	Buffeting During Atmospheric Ascent, May 1964 – Revised November 1970
SP-8002	(Structures)	Flight-Loads Measurements During Launch and Exit, December 1964
SP-8003	(Structures)	Flutter, Buzz, and Divergence, July 1964
SP-8004	(Structures)	Panel Flutter, July 1964
SP-8005	(Environment)	Solar Electromagnetic Radiation, June 1965 – Revised May 1971
SP-8006	(Structures)	Local Steady Aerodynamic Loads During Launch and Exit, May 1965
SP-8007	(Structures)	Buckling of Thin-Walled Circular Cylinders, September 1965 – Revised August 1968
SP-8008	(Structures)	Prelaunch Ground Wind Loads, November 1965
SP-8009	(Structures)	Propellant Slosh Loads, August 1968
SP-8010	(Environment)	Models of Mars Atmosphere (1967), May 1968
SP-8011	(Environment)	Models of Venus Atmosphere (1968), December 1968
SP-8012	(Structures)	Natural Vibration Modal Analysis, September 1968
SP-8013	(Environment)	Meteoroid Environment Model – 1969 [Near Earth to Lunar Surface], March 1969
SP-8014	(Structures)	Entry Thermal Protection, August 1968
SP-8015	(Guidance and Control)	Guidance and Navigation for Entry Vehicles, November 1968
SP-8016	(Guidance and Control)	Effects of Structural Flexibility on Spacecraft Control Systems, April 1969
SP-8017	(Environment)	Magnetic Fields – Earth and Extraterrestrial, March 1969
SP-8018	(Guidance and Control)	Spacecraft Magnetic Torques, March 1969
SP-8019	(Structures)	Buckling of Thin-Walled Truncated Cones, September 1968
SP-8020	(Environment)	Mars Surface Models (1968), May 1969
SP-8021	(Environment)	Models of Earth's Atmosphere (120 to 1000 km), May 1969

SP-8022	(Structures)	Staging Loads, February 1969
SP-8023	(Environment)	Lunar Surface Models, May 1969
SP-8024	(Guidance and Control)	Spacecraft Gravitational Torques, May 1969
SP-8025	(Chemical Propulsion)	Solid Rocket Motor Metal Cases, April 1970
SP-8026	(Guidance and Control)	Spacecraft Star Trackers, July 1970
SP-8027	(Guidance and Control)	Spacecraft Radiation Torques, October 1969
SP-8028	(Guidance and Control)	Entry Vehicle Control, November 1969
SP-8029	(Structures)	Aerodynamic and Rocket-Exhaust Heating During Launch and Ascent, May 1969
SP-8030	(Structures)	Transient Loads from Thrust Excitation, February 1969
SP-8031	(Structures)	Slosh Suppression, May 1969
SP-8032	(Structures)	Buckling of Thin-Walled Doubly Curved Shells, August 1969
SP-8033	(Guidance and Control)	Spacecraft Earth Horizon Sensors, December 1969
SP-8034	(Guidance and Control)	Spacecraft Mass Expulsion Torques, December 1969
SP-8035	(Structures)	Wind Loads During Ascent, June 1970
SP-8036	(Guidance and Control)	Effects of Structural Flexibility on Launch Vehicle Control Systems, February 1970
SP-8037	(Environment)	Assessment and Control of Spacecraft Magnetic Fields, September 1970
SP-8038	(Environment)	Meteoroid Environment Model – 1970 (Interplanetary and Planetary), October 1970
SP-8040	(Structures)	Fracture Control of Metallic Pressure Vessels, May 1970
SP-8041	(Chemical Propulsion)	Captive-Fired Testing of Solid Rocket Motors, March 1971
SP-8042	(Structures)	Meteoroid Damage Assessment, May 1970
SP-8043	(Structures)	Design-Development Testing, May 1970
SP-8044	(Structures)	Qualification Testing, May 1970
SP-8045	(Structures)	Acceptance Testing, April 1970
SP-8046	(Structures)	Landing Impact Attenuation for Non-Surface-Planing Landers, April 1970
SP-8047	(Guidance and Control)	Spacecraft Sun Sensors, June 1970

SP-8048	(Chemical Propulsion)	Liquid Rocket Engine Turbopump Bearings, March 1971
SP-8050	(Structures)	Structural Vibration Prediction, June 1970
SP-8051	(Chemical Propulsion)	Solid Rocket Motor Igniters, March 1971
SP-8053	(Structures)	Nuclear and Space Radiation Effects on Materials, June 1970
SP-8054	(Structures)	Space Radiation Protection, June 1970
SP-8055	(Structures)	Prevention of Coupled Structure-Propulsion Instability (Pogo), October 1970
SP-8056	(Structures)	Flight Separation Mechanisms, October 1970
SP-8057	(Structures)	Structural Design Criteria Applicable to a Space Shuttle, January 1971
SP-8058	(Guidance and Control)	Spacecraft Aerodynamic Torques, January 1971
SP-8059	(Guidance and Control)	Spacecraft Attitude Control During Thrusting Maneuvers, February 1971
SP-8060	(Structures)	Compartment Venting, November 1970
SP-8061	(Structures)	Interaction with Umbilicals and Launch Stand August 1970
SP-8062	(Structures)	Entry Gasdynamic Heating, January 1971
SP-8063	(Structures)	Lubrication, Friction, and Wear, June 1971
SP-8066	(Structures)	Deployable Aerodynamic Deceleration Systems, June 1971
SP-8068	(Structures)	Buckling Strength of Structural Plates, June 1971
SP-8072	(Structures)	Acoustic Loads Generated by the Propulsion System, June 1971

NASA-Langley, 1971 —— 32